

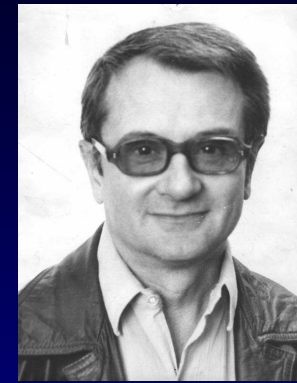
MACROSCOPIC-MICROSCOPIC METHOD FOR ATOMIC CLUSTER PHYSICS



OUTLINE

- Macroscopic-microscopic approach
- Experimental shapes of deposited clusters and mass spectrum of free clusters
- Liquid drop model of metallic clusters (binding and deformation energy)
 - Neutral free spheroidal Na cluster
 - Hemisphere and Hemispheroidal shapes
 - Simulating the interaction with the surface
 - Short and long spheroidal caps
- Deformed single particle shell models
 - Spheroidal harmonic oscillator
 - Hemispheroidal harmonic oscillator
 - Influence of the I^2 term
- Microscopic shell and pairing corrections
- Equilibrium shapes of Na clusters
- Conclusions

Liquid Drop Model + corrections



John William Strutt (**Lord Rayleigh**), Phil. Mag. **14** (1878) 184: Capillarity instability of a jet of fluid.

Niels Bohr, Nature **137** (1936) 344: LDM applied to atomic nuclei

Explained the induced nuclear fission:

- **Lise Meitner** and O. Frisch, Nature **143** (1939) 239
- N. Bohr and J. Wheeler, Phys. Rev. **56** (1939) 426

V.M. Strutinsky Nucl. Phys. A **95** (1967) 420: shell+pairing corrections. Since 1967, the Macroscopic-Microscopic method successfully used in Nuclear Physics.

Adapted to atomic cluster physics in the 90s.

Macroscopic-microscopic meth.

LDM is suitable since delocalized conduction electrons of a metallic cluster form a Fermi liquid like the atomic nucleus.

- Macroscopic Liquid Drop Model: E_{LD}
- Single-particle shell model (SPSM): energy levels vs. deformation time consuming computations
- Shell + pairing correction method: $\delta E = \delta U + \delta P$
- Total deformation energy: $E_{def} = E_{LD} + \delta E$

for a given parametrization of the drop surface $\rho = \rho(z)$. The potential part of SPSM Hamiltonian should admit $\rho = \rho(z)$ as an equipotential surface.

For deposited clusters we choose the **hemispheroidal shape**, allowing to obtain analytical results.

Compare M-MA: nuclei & AC

Orders of magnitude for a Na cluster. $1 \text{ \AA} = 0.1 \text{ nm}$.

Quantity	Nucleus	Atomic Cluster	Ratio N/A
Binding Energy	8 MeV/nucleon	2 eV/atom	$4 \cdot 10^6$
Radius constant	1.16 fm	2.117 Å	$5 \cdot 10^{-6}$
Shell gap $\hbar\omega_0$ for A or n =125	8.2 MeV	0.61 eV	$1.3 \cdot 10^7$

For a neutral atomic cluster there is no Coulomb energy. The curvature energy should be taken into account. When we calculate microscopic corrections for a nucleus we have to consider separately the level schemes of protons and neutrons.

Cluster shapes and volumes

Cylindrical symmetry.

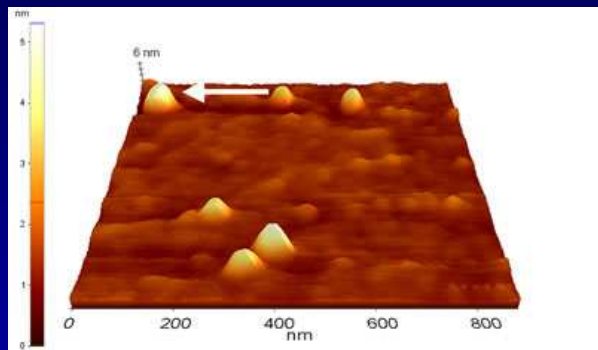
- sphere, $V_{ol}^0 = 4\pi R_0^3/3$, $R_0 = r_s N^{1/3}$
- spheroid, $V_{ol}^0 = 4\pi a^2 c R_0^3/3$
- hemisphere, $V_{ol}^s = 2\pi R_s^3/3$, $R_s = 2^{1/3} R_0$
- hemispheroid, $V_{ol}^s = 2\pi a^2 c R_s^3/3$
- short spheroidal cap ($h = c - d$),
 $V(\delta) = \pi R_{sc}^3 h^2 \frac{a^2}{3c^2} (3c - h)$, $R_{sc} = 4^{1/3} R_0 [h_0^2 (3 - h_0)]^{-1/3}$
- long spheroidal cap ($h = c + d$),
 $V(\delta) = \pi R_{sc}^3 h^2 \frac{a^2}{3c^2} (3c - h)$

Equilibrium shapes — minima of deformation energy.

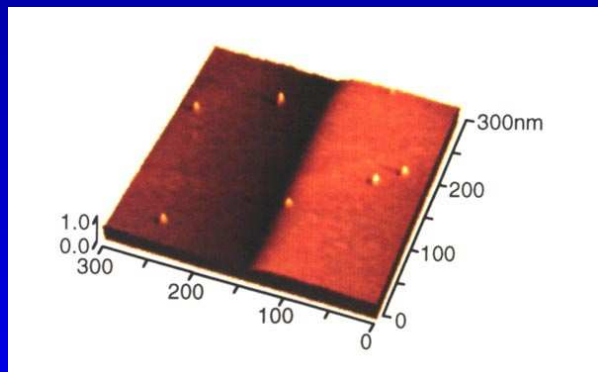
FEW EXPERIMENTAL FACTS

Prolate clusters on a surface

Ultrasensitive microscopy: Scanning tunneling microscope (STM) — 1981 Gerd Binnig and Heinrich Rohrer (Nobel Prize 1986). Atomic Force Microscope (AFM), etc.

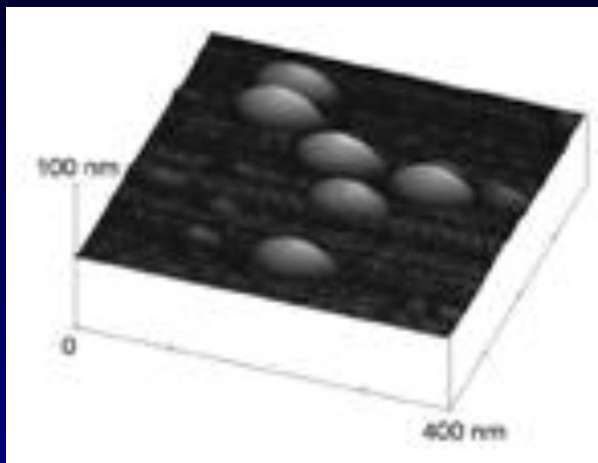


Au colloids deposited on a special glass. B. Bonanni and S. Cannistraro, *J. Nanotechnology Online*, Nov. 11, 2005. DOI: 10.2240/azojono0105.

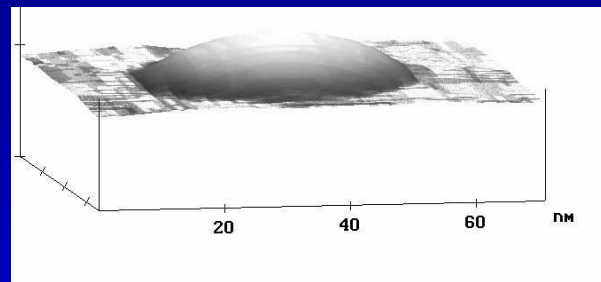


Clusters projected with energy close to the threshold stay at the impact point. Loughborough University & University of Birmingham.

Oblate clusters on a surface

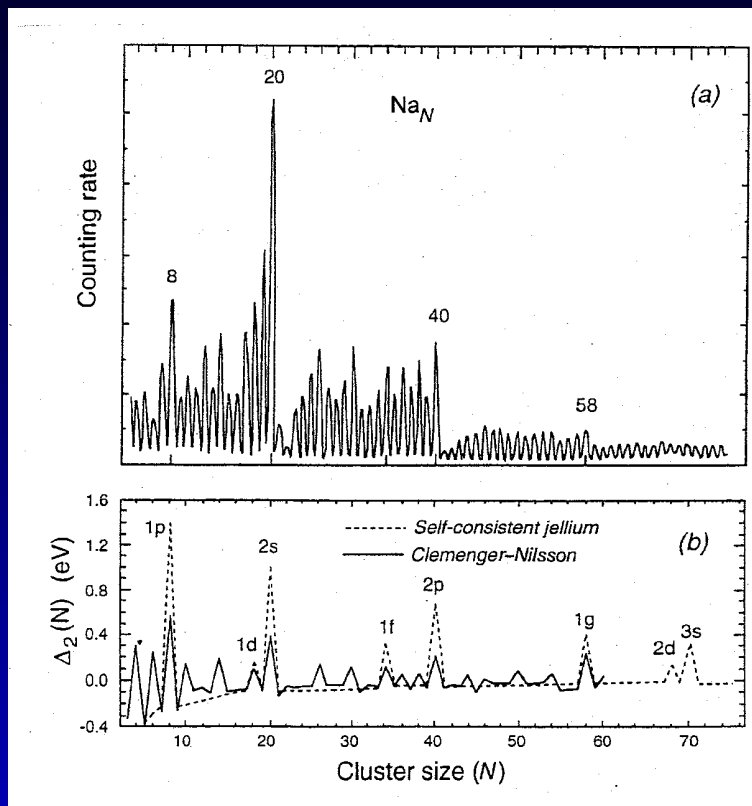


AFM image of Bi clusters supported on a SiO_2 surface. J.C. Partridge, S.A. Brown *et al.*, *Phys. Stat. Sol. (a)* **203** (2006) 1217



One of the cluster from the above figure. Simon A. Brown, private communication, 2008

Mass spectrum Na free clust.



(a) Mass spectrum detected with a quadrupole mass analyser.
Major peaks at **8, 20, 40, 58**.

(b) Calculated 2nd differences in total electronic energies.

Next magic numbers: **92, 136, 198, 264, 344, 442, ...**

From W. D. Knight *et al.* *Phys. Rev. Lett.* **52** (1984) 2141–2143.

NEUTRAL FREE SPHEROIDAL NA CLUSTER

Binding en., spherical Na clusters

$$E_N = \alpha_v N + \alpha_s N^{2/3} + \alpha_c N^{1/3}$$

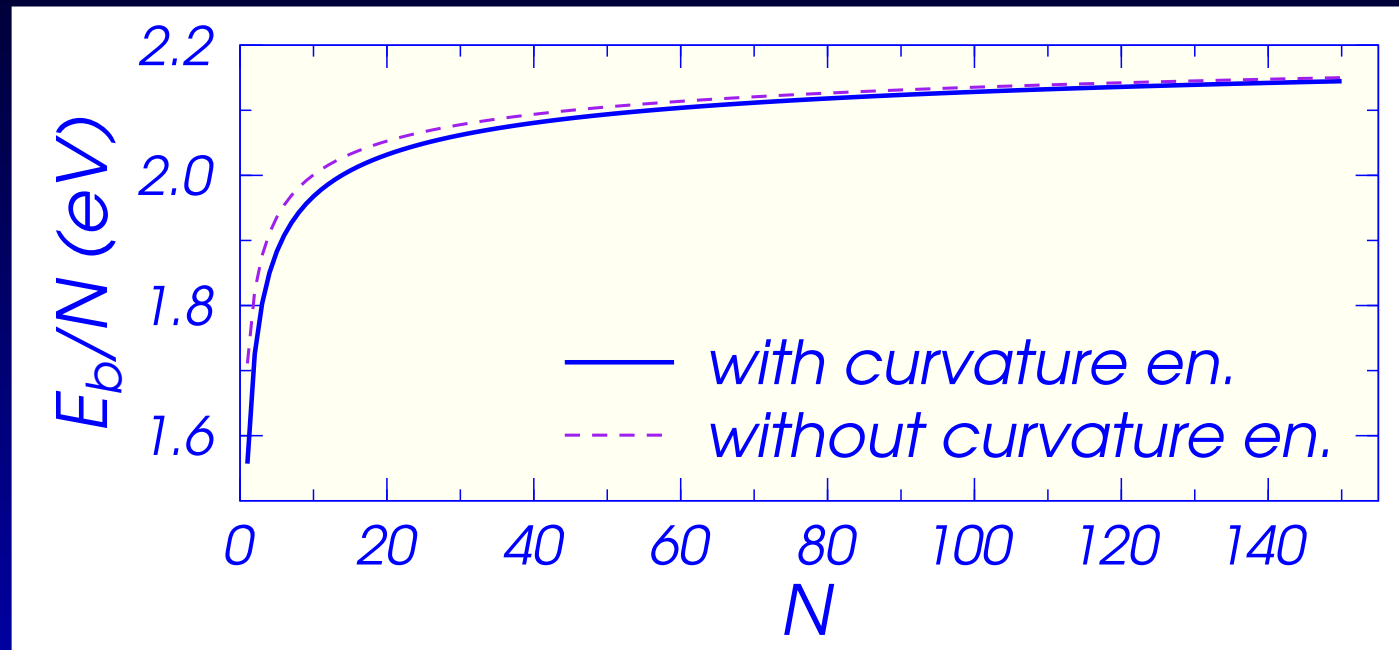


Fig: Binding energy per atom ($-E_b/N$)

Material properties: volume, surface, curvature coeff. of Na

$\alpha_v = -2.252$, $\alpha_s = 0.541$, $\alpha_c = 0.154$, determined by fitting the Extended Thomas-Fermi-LDA for spherical shapes.

(C. Yannouleas, U. Landman, *Phys. Rev. B* **51** (1995) 1902)

Geometry and material properties

Energies in eV for Na (monovalent) spherical cluster with N atoms

$$E_v^0 = -2.252N$$

Volume energy is proportional to the volume.

$$E_s^0 = 0.541N^{2/3}$$

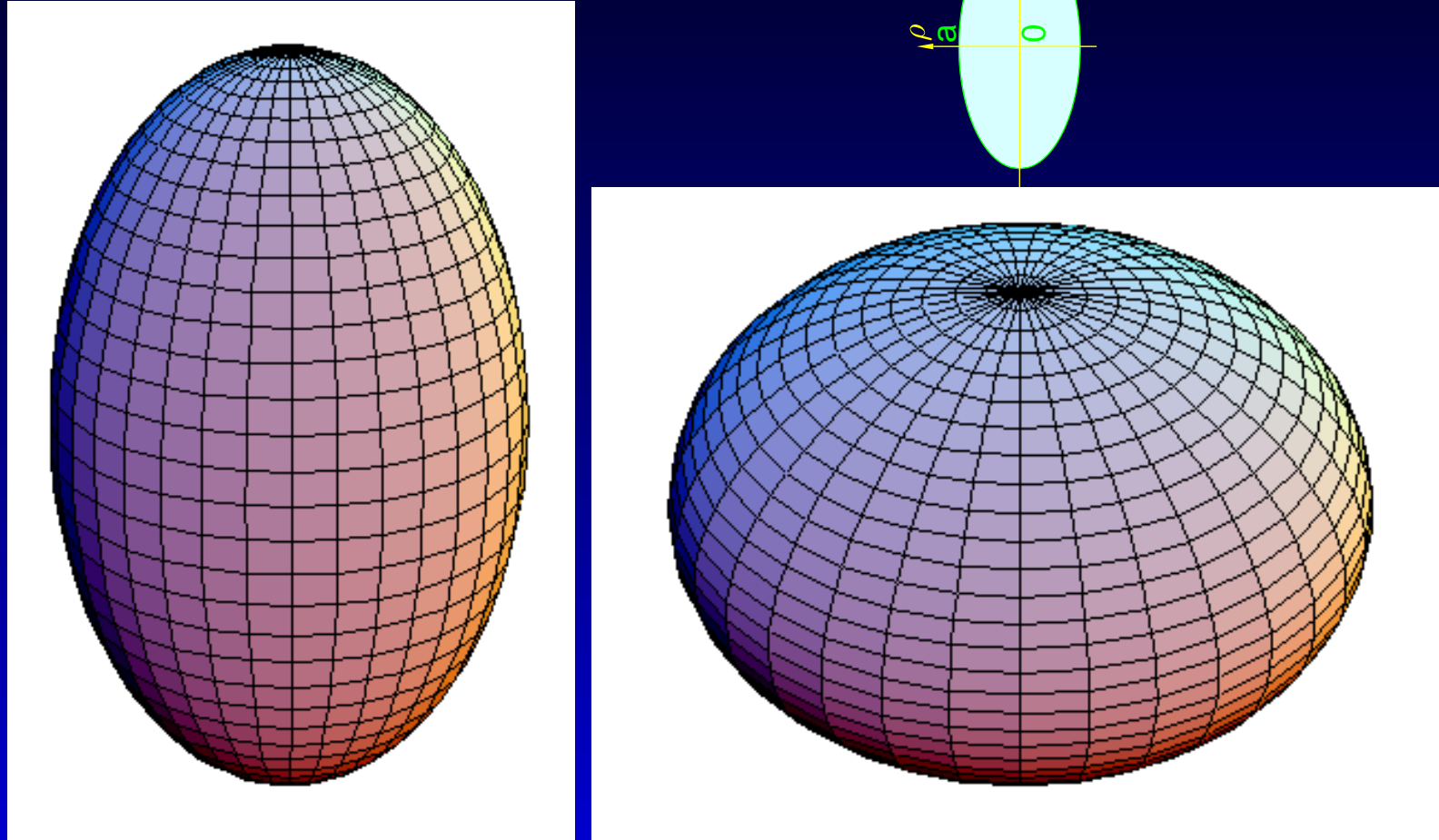
Surface energy is proportional to the surface area and to the surface tension σ : $E_s^0 = 4\pi R_0^2 \sigma = 4\pi r_s^2 \sigma N^{2/3}$, $4\pi r_s^2 \sigma = 0.541$ eV

$$E_{curv}^0 = 0.154N^{1/3}$$

Curvature energy is proportional to the integrated curvature, $K_0 = \int dS \kappa = 4\pi R_0$, and to the curvature tension γ_c :

$$E_{curv}^0 = 4\pi R_0 \gamma_c = 4\pi r_s \gamma_c N^{1/3}$$
, $4\pi r_s \gamma_c = 0.154$ eV

Prolate & oblate spheroids



$$\frac{\rho^2}{a^2} + \frac{z^2}{c^2} = 1 \quad \rho^2 = x^2 + y^2 \quad a^2 c = 1$$

Spheroidal deformation

Spheroidal deformation δ

$\delta < 0$ oblate $\delta > 0$ prolate

(K.L. Clemenger, PhD Thesis, Univ. of California, Berkeley, 1985)

Dimensionless semiaxes (units of $R_0 = r_s N^{1/3}$ for spheroid and of $R_s = 2^{1/3} R_0$) for hemispheroid

$$a = \left(\frac{2 - \delta}{2 + \delta} \right)^{1/3} ; \quad c = \left(\frac{2 + \delta}{2 - \delta} \right)^{2/3}$$

$$\frac{a}{c} = \frac{2 - \delta}{2 + \delta} = a^3$$

r_s – Wigner-Seitz radius. N – number of atoms
(delocalized conduction electrons)

LDM for spheroidal Na cluster

Volume is conserved. The vol. energy is independent on deformation.

Deformation energy with respect to spherical shape (surface + curvature)

$$E - E^0 = (E_s - E_s^0) + (E_c - E_c^0)$$

$$E - E^0 = E_s^0 \left(\frac{E_s}{E_s^0} - 1 \right) + E_c^0 \left(\frac{E_c}{E_c^0} - 1 \right)$$

$$E - E^0 = E_s^0 (B_{surf} - 1) + E_c^0 (B_{curv} - 1)$$

Dimensionless deformation-dependent terms:

$$B_{surf}, B_{curv}$$

Cylindrically symmetric shapes

The deformation-dependent surface and curvature energies for cylindrical symmetry (surface equation $\rho = \rho(z)$ with $-c, +c$ tips on z -axis and $\rho' = d\rho/dz$, $\rho'' = d^2\rho/dz^2$) are

$$B_{surf} = \frac{S}{4\pi R_0^2} = \frac{1}{2} \int_{-c}^{+c} dz \rho \sqrt{1 + \rho'^2} = \frac{1}{2} \int_{-c}^{+c} dz \sqrt{\rho^2 + (\rho\rho')^2}$$

$$B_{curv} = \frac{1}{4\pi R_0} \int dS \kappa = \frac{1}{4} \int_{-c}^{+c} dz \frac{1 + \rho'^2 - \rho\rho''}{1 + \rho'^2}$$

The local curvature $\kappa = 0.5(\mathcal{R}_1^{-1} + \mathcal{R}_2^{-1})$ where the principal radii of curvature (D.N. Poenaru, R.A. Gherghescu, W. Greiner, *Nucl. Phys. A 747 (2005) 182*)

$$\mathcal{R}_1 = R_0 \rho \sqrt{1 + \rho'^2} \quad \mathcal{R}_2 = -R_0 (1 + \rho'^2)^{3/2} / \rho''$$

Energies of spheroidal shapes

$$B_{surf} = \frac{a}{2c^2} \int_{-c}^{+c} dz \sqrt{c^4 + z^2(a^2 - c^2)}$$

$$B_{curv} = \frac{c}{2} + \frac{a^2 c^2}{4} \int_{-c}^{+c} \frac{dz}{c^4 + z^2(a^2 - c^2)} = \frac{c}{2} + \frac{c}{4} \int_{-c}^{+c} \frac{dz}{c^4 + z^2(a^2 - c^2)}$$

Oblate ($a > c$, eccentricity $e = \sqrt{a^2/c^2 - 1}$):

$$B_{surf} = \frac{a}{2} \left(a + \frac{c}{2e} \ln \frac{a + ce}{a - ce} \right) \quad B_{curv} = \frac{c}{2} + \frac{a^2}{2ce} \arctan e$$

Misprint in formula of B_{surf} in a book by Hasse & Myers, Geometrical ... (Springer,1988).

Correct in Beringer & Knox, Phys. Rev. 121 (1961) 1195.

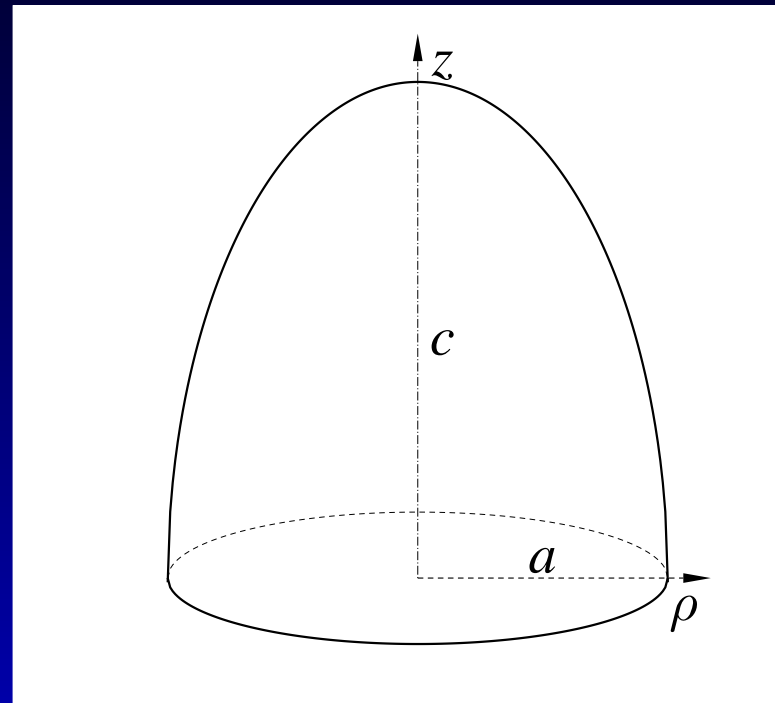
Prolate ($a < c$, eccentricity $e = \sqrt{1 - a^2/c^2}$):

$$B_{surf} = \frac{a}{2} \left(a + \frac{c}{e} \arcsin e \right) \quad B_{curv} = \frac{c}{2} + \frac{a^2}{4ec} \ln \left| \frac{1+e}{1-e} \right|$$

NEUTRAL HEMISPHEROIDAL NA CLUSTER ON A PLANAR SURFACE

Surface parametrization

Hemispheroid with z-axis \perp on the surface plane



$$\rho^2 = \begin{cases} (a/c)^2(c^2 - z^2) & z \geq 0 \\ 0 & z < 0 \end{cases}$$

$c > a$ – **prolate**

$c < a$ – **oblate**

Binding en. of hemisph. clusters

Volume: 1)sphere $V_{ol}^0 = 4\pi a^2 c R_0^3 / 3$;

2)hemisphere $V_{ol}^s = 2\pi a^2 c R_s^3 / 3$

$$R_s = 2^{1/3} R_0$$

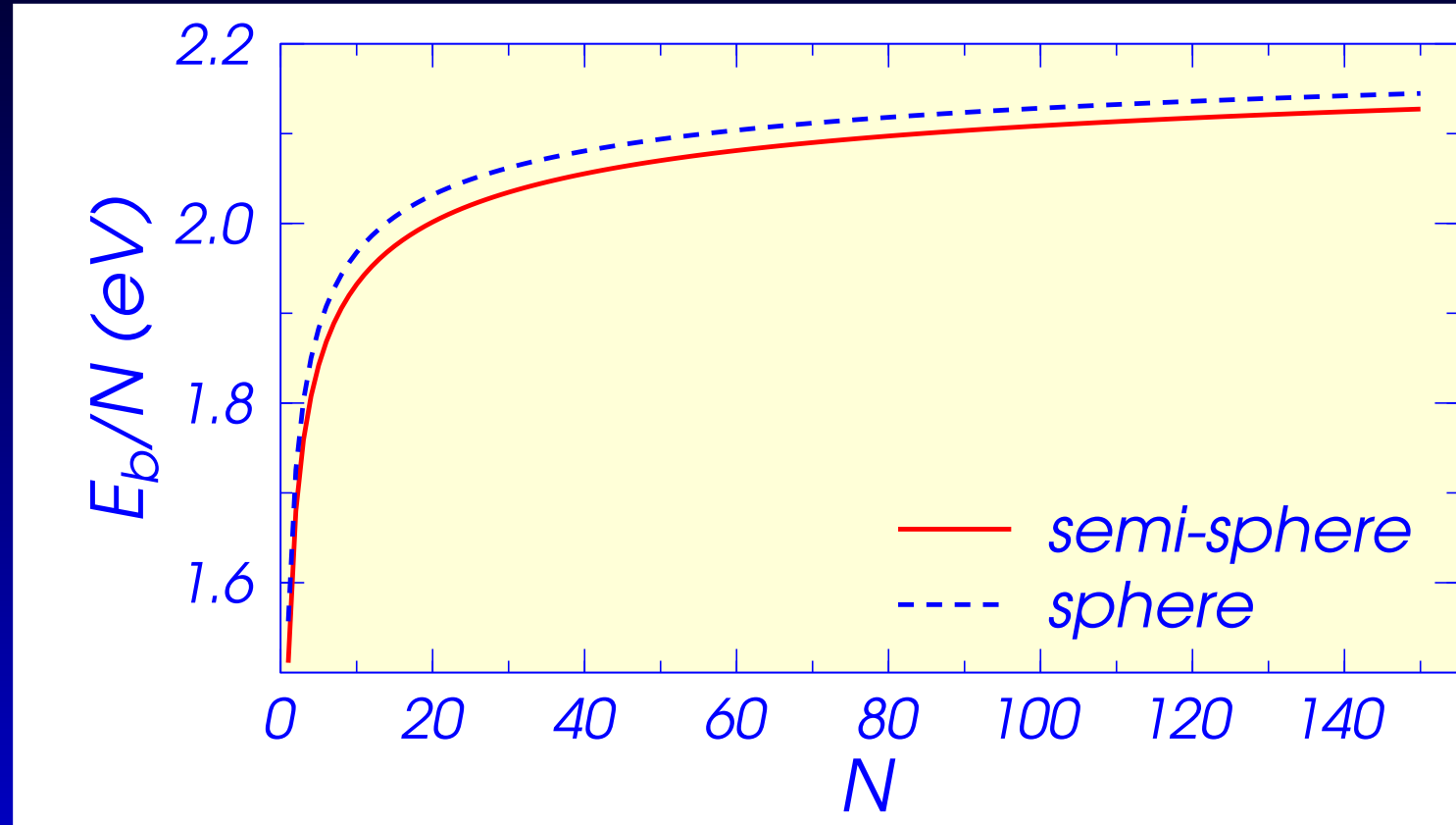
$$E - E^{s0} = E_s^{s0} (B_{surf}^s - 1) + E_c^{s0} (B_{curv}^s - 1)$$

$$E_s^{s0} = (3/4^{2/3}) E_s^0 ; \quad E_c^{s0} = E_{curv}^0 / 4^{1/3}$$

Binding energy for Na hemispherical cluster with N atoms:

$$E_{sN} = -2.252N + \frac{3}{4^{2/3}} 0.541N^{2/3} + \frac{1}{4^{1/3}} 0.154N^{1/3}$$

Binding energy for Na clusters



Binding energy per atom ($-E_b/N$) versus the number of atoms N for Na clusters. Hemisphere & sphere.

Def. en. hemisph. clusters

Oblate ($a > c$) hemispheroid, $e^2 = a^2/c^2 - 1$

$$B_{surf}^s = \frac{a}{3} \left[2a + \frac{c}{e} \ln \left(e + \frac{a}{c} \right) \right]$$

$$B_{curv}^s = \frac{c}{2} + \frac{a^2}{2ce} \arctan e$$

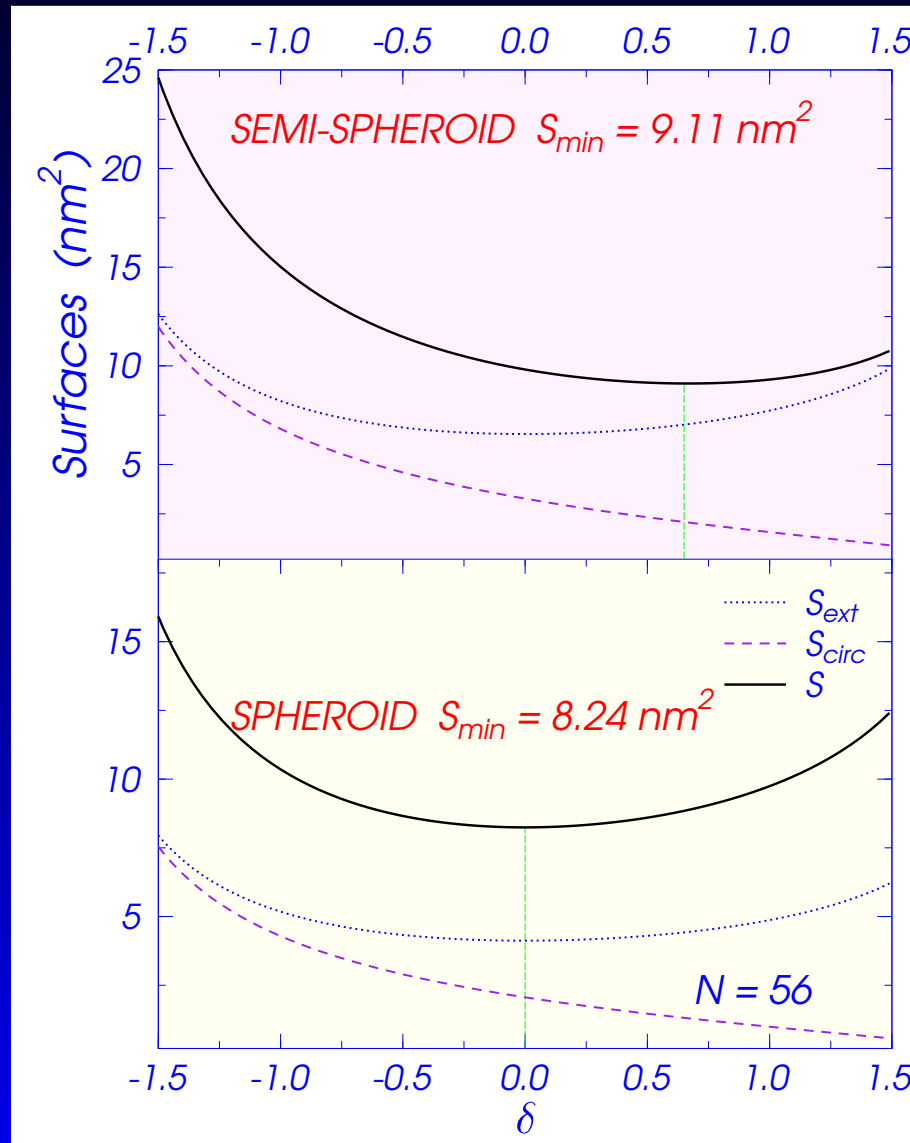
Prolate ($c > a$) hemispheroid, $e^2 = 1 - a^2/c^2$

$$B_{surf}^s = \frac{a}{3} \left(2a + \frac{c}{e} \arcsin e \right)$$

$$B_{curv}^s = \frac{c}{2} + \frac{a^2}{4ce} \ln \left| \frac{1+e}{1-e} \right|$$

Surface area of Na_{56} cluster

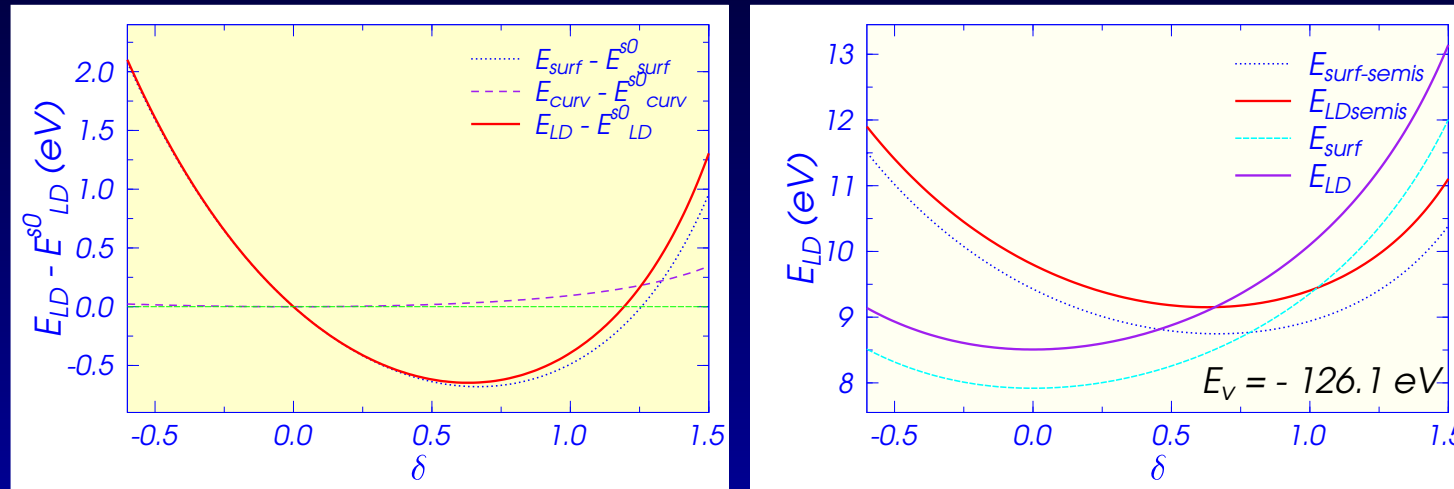
Liquid drop stability



The spherical shape is the most stable for a spheroid.

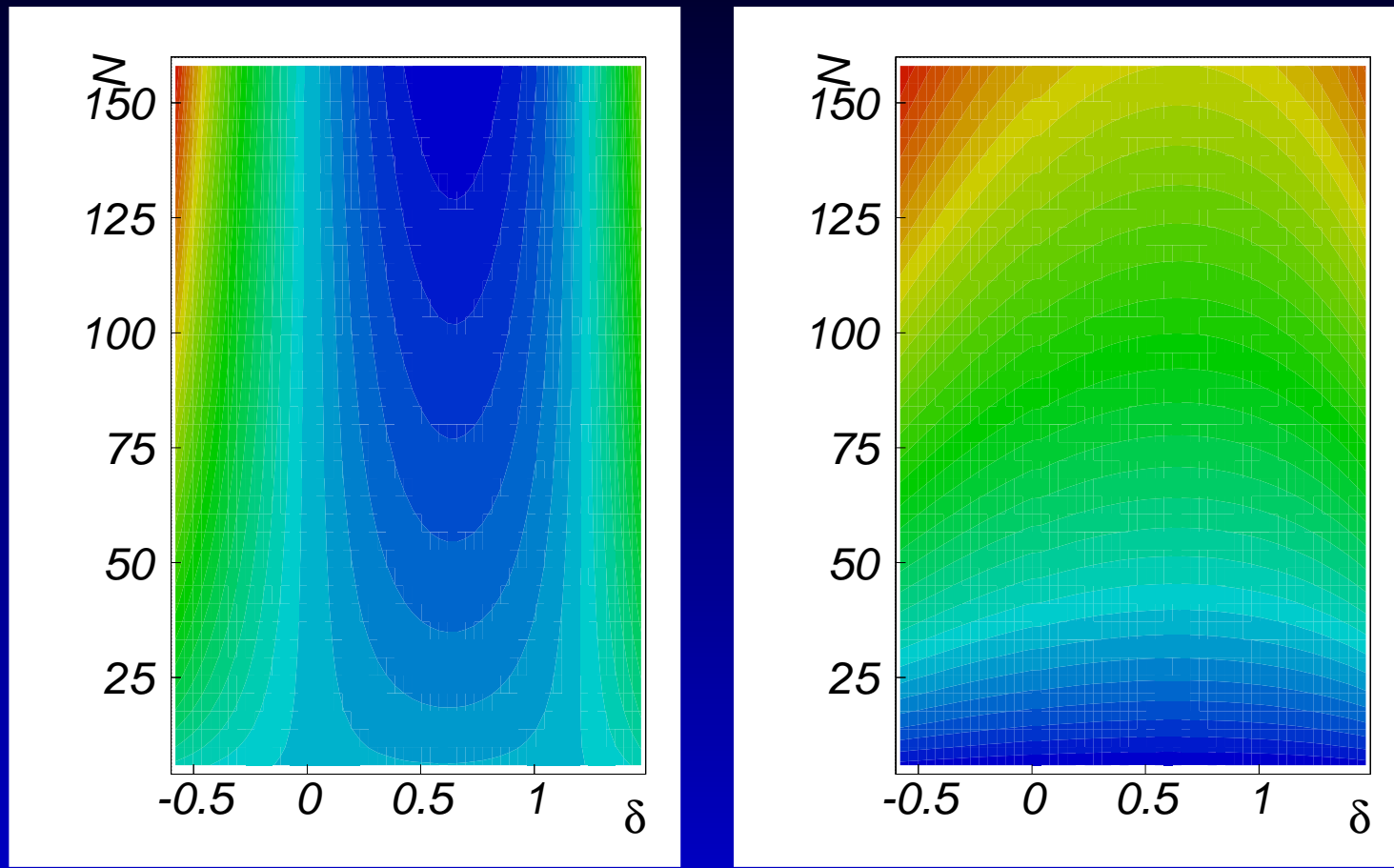
The prolate superdeformed shape is the most stable for a hemispheroid because the surface of a circular base is decreasing with deformation while the external area is smaller at $\delta = 0$.

LDM hemisph. Na₅₆ cluster



Surface plus curvature deformation energy with respect to a hemisphere and absolute values. The minimum is around the supereformed prolate shape with $\delta = 0.65$ ($c/a = 1.96$), unlike for a spheroid ($\delta = 0$).

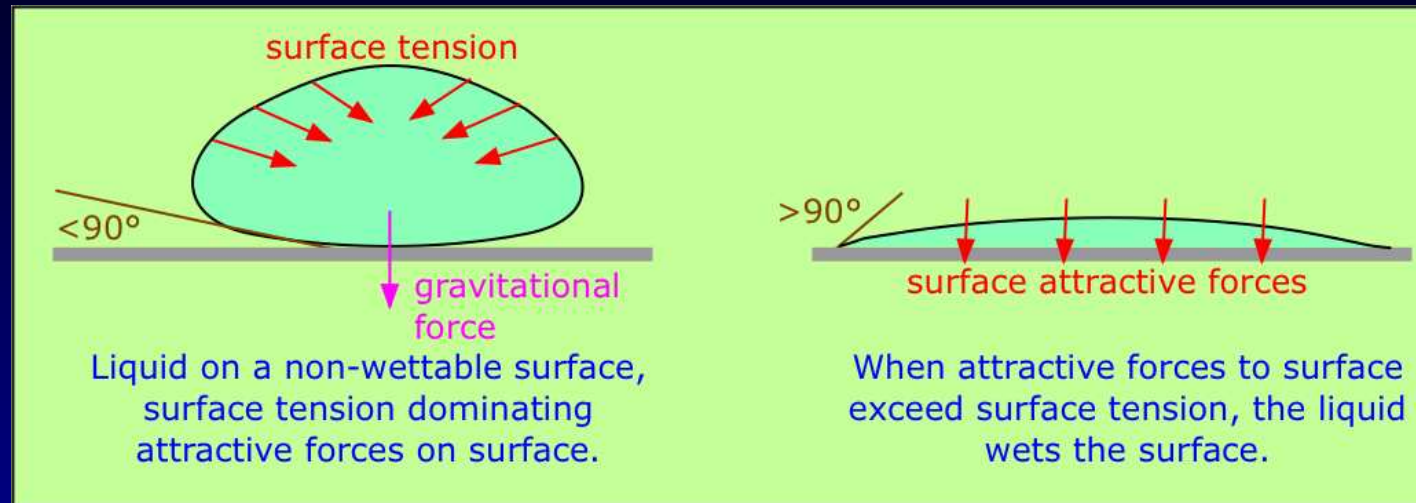
Surface + curvature energy



Deformation energy contour plot with respect to a hemisphere and absolute values. Equilibrium for superdeformed prolate shape at all N .

SIMULATING THE INTERACTION WITH THE SURFACE

Water droplet - LDM



In contact with a solid the liquid behavior depends on the surface tension σ and the attractive forces between the molecules of the liquid and of solid. If an H_2O molecule is more strongly attracted to its own kind, then σ will dominate, increasing the curvature of the interface. A clean glass surface has $-\text{OH}$ groups which attach to water molecules through hydrogen bonding; this causes the water to wet the surface. A detergent added to water reduces σ .

Simulating the interaction

Surface tension of the base is changed **from σ to $i\sigma$** ,
 $i \in (-1.98, 2)$. i is the *interaction factor*.

For $i = 1$ one has the previously studied case:

Our group, EPL 79 (2007) 63001;

EPJD (2008) online, doi: 10.1140/epjd/e2008-00066-6 → HIGHLIGHT PAPER

$$E = E_{base} + E_{ext} = i\sigma S_{base} + \sigma S_{ext}$$

The curvature of a planar surface is zero, hence E_{curv} remains unchanged. For $\delta = 0$ (hemisphere):

$$E_s^{si0} = i\sigma(\pi R_s^2) + \sigma(2\pi R_s^2) = 4^{-2/3}(2+i)E_s^0$$

$$E_c^{si0} = 2\pi R_s \gamma_c = 4^{-1/3} E_{curv}^0$$

Deformation energy analytical rel.

With respect to hemispherical shape

$$E^{si} - E^{si0} = E_s^{si0} (B_{surf}^{si} - 1) + E_c^{si0} (B_{curv}^{si} - 1)$$

Oblate hemispheroid ($a > c$, $e^2 = a^2/c^2 - 1$)

$$B_{surf}^{si} = \frac{i}{2+i} a^2 + \frac{1}{2+i} \left[a^2 + \frac{ac}{e} \ln \left(e + \frac{a}{c} \right) \right]$$

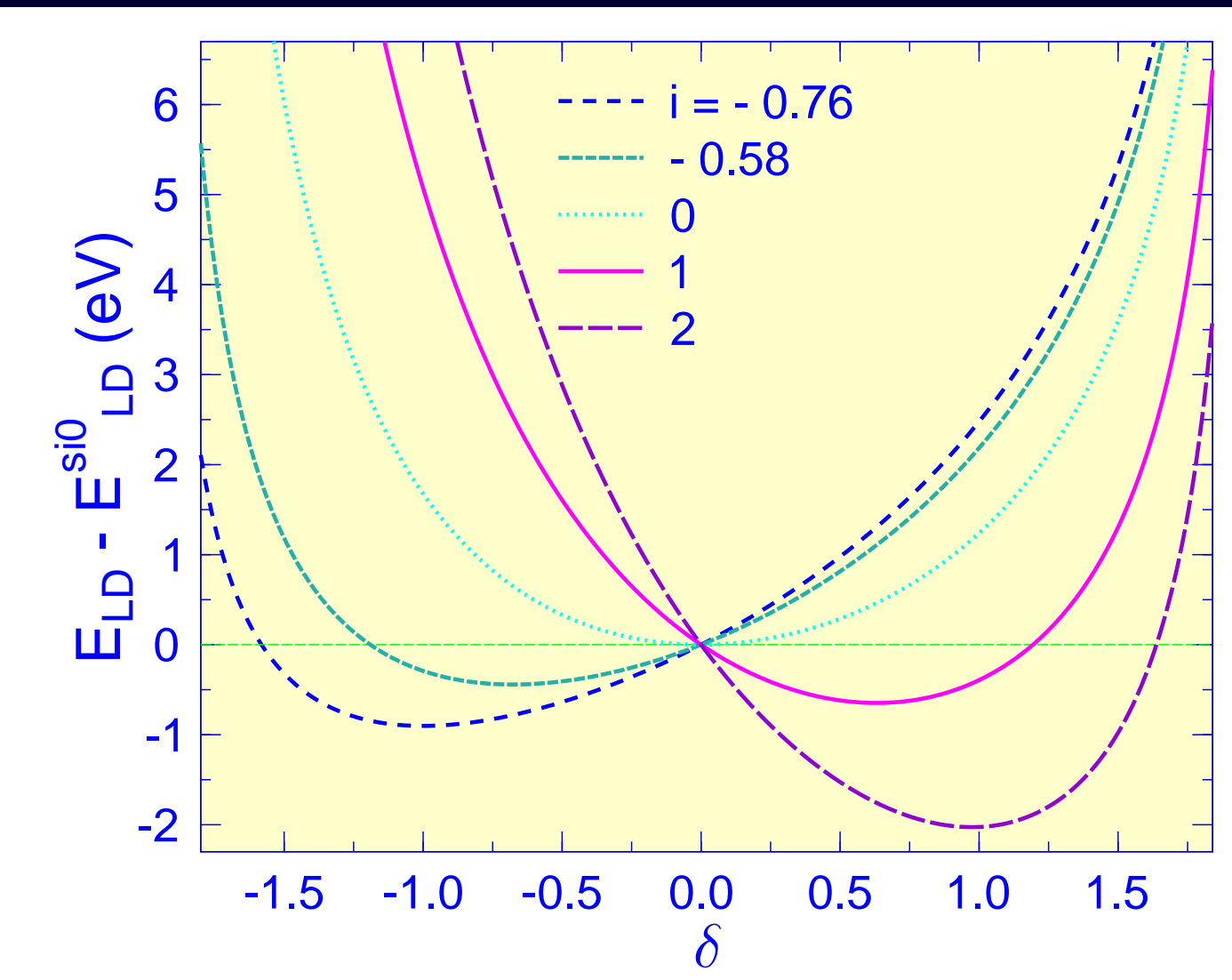
$$B_{curv}^{si} = B_{curv}^s = \frac{c}{2} + \frac{a^2}{2ce} \arctan e$$

Prolate hemispheroid ($c > a$, $e^2 c^2 = c^2 - a^2$)

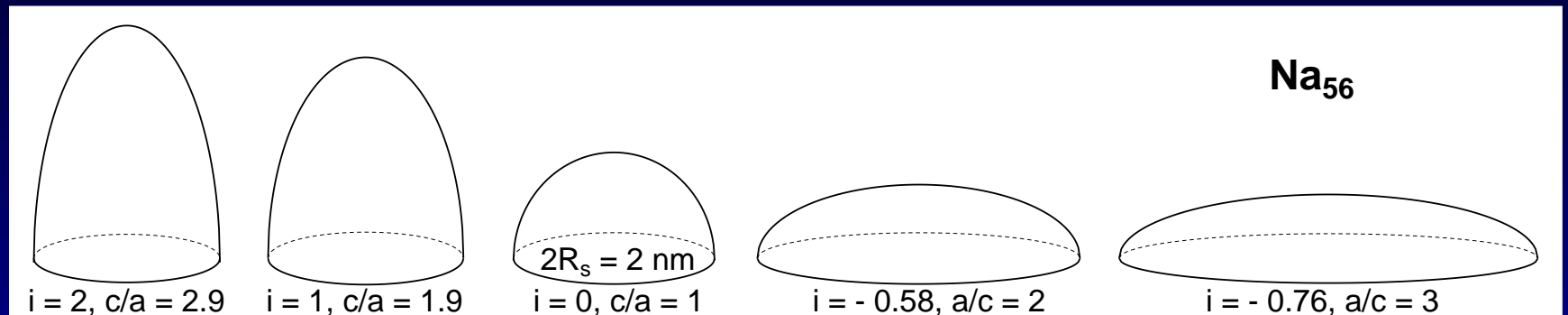
$$B_{surf}^{si} = \frac{i}{2+i} a^2 + \frac{1}{2+i} \left[a^2 + \frac{ac}{e} \arcsin e \right]$$

$$B_{curv}^{si} = B_{curv}^s = \frac{c}{2} + \frac{a^2}{4ce} \ln \left| \frac{1+e}{1-e} \right|$$

Minima of deformation energy, Na_{56}



Equilibrium shapes of Na₅₆



$i = 2$ hyperdeformed prolate

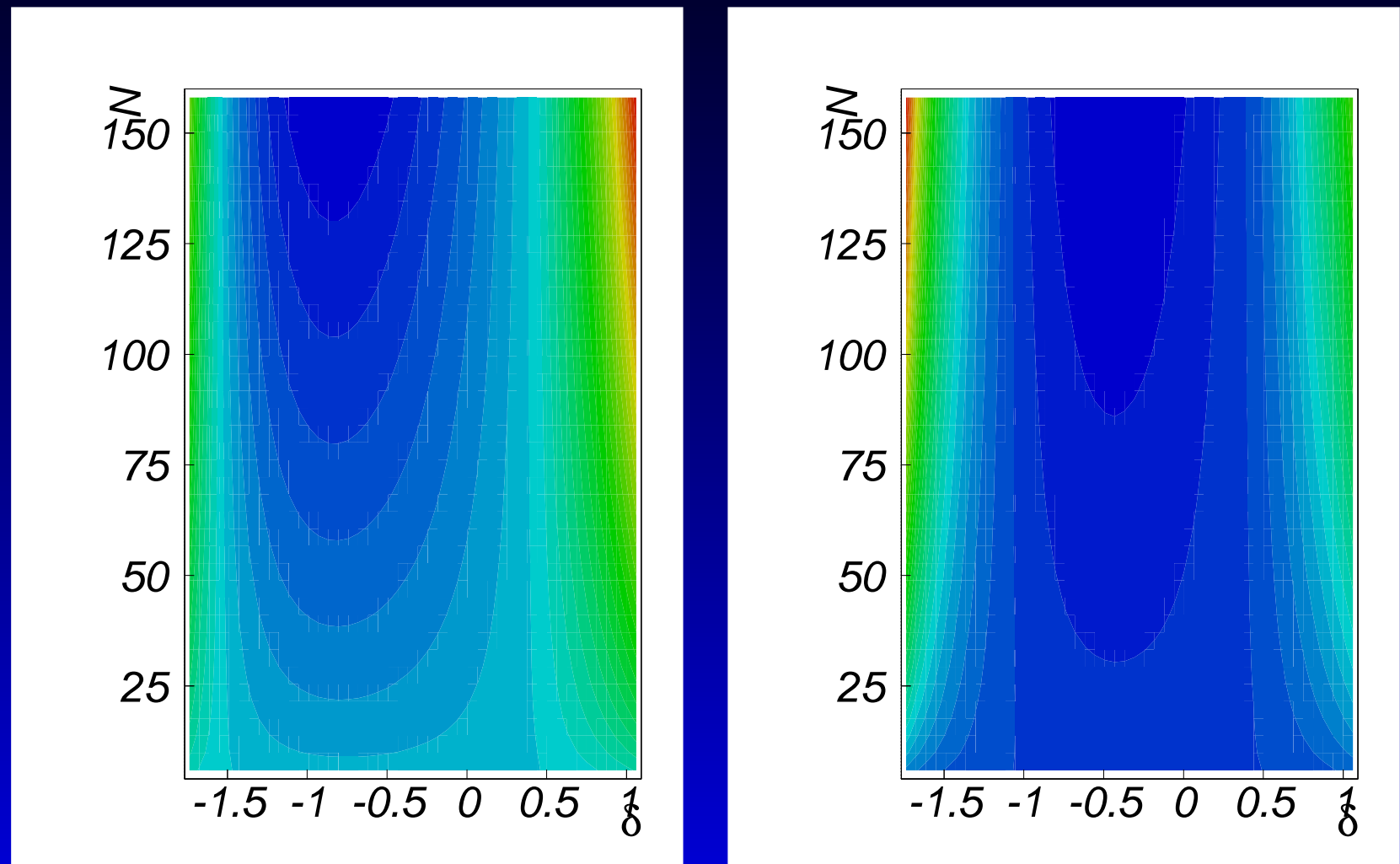
$i = 1$ superdeformed prolate

$i = 0$ hemisphere

$i = -0.58$ superdeformed oblate

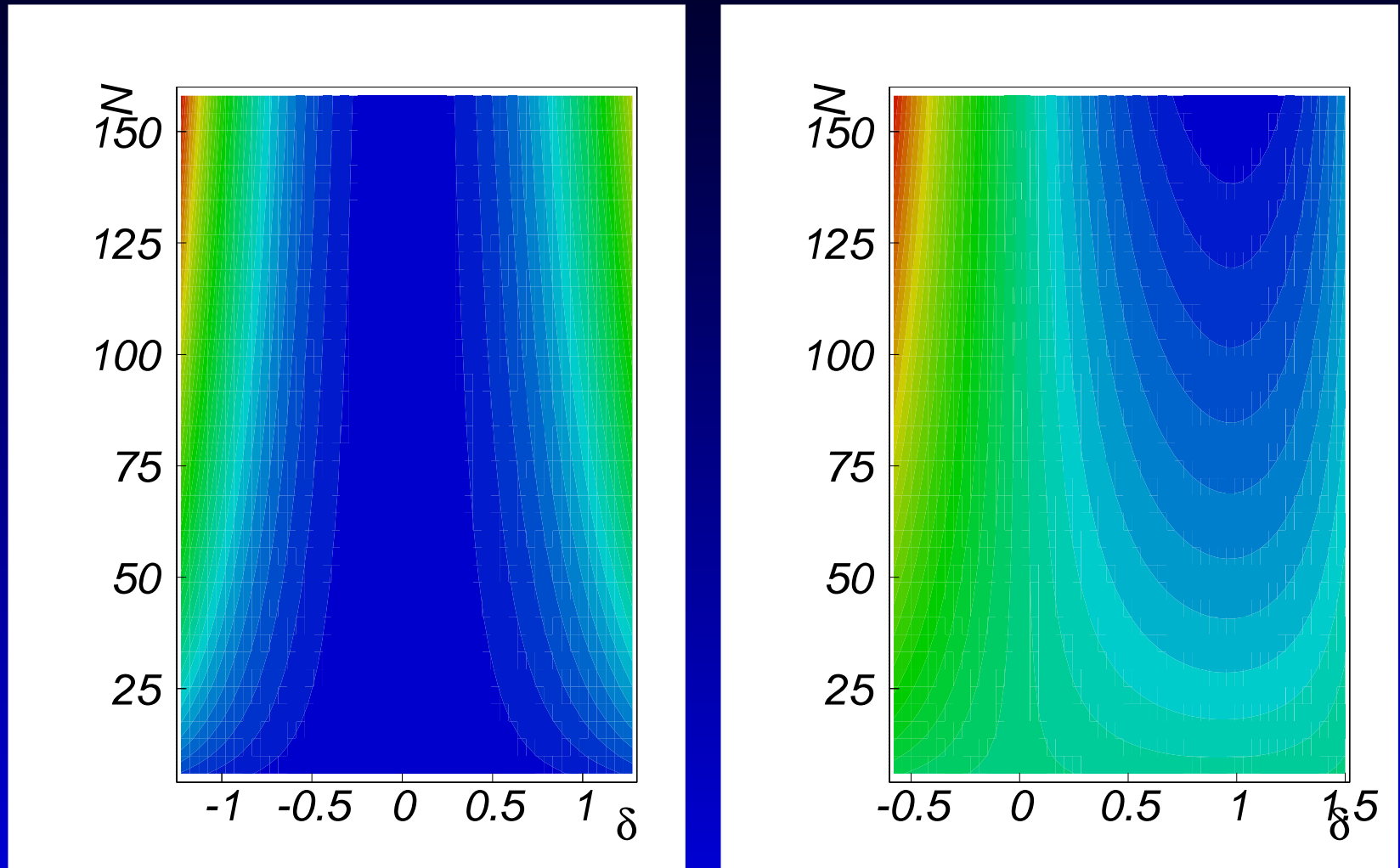
$i = -0.76$ hyperdeformed oblate.

Contour pl E_{LDrel} , $\mathbf{i} = -0.76, -0.58$



Minima practically independent on N

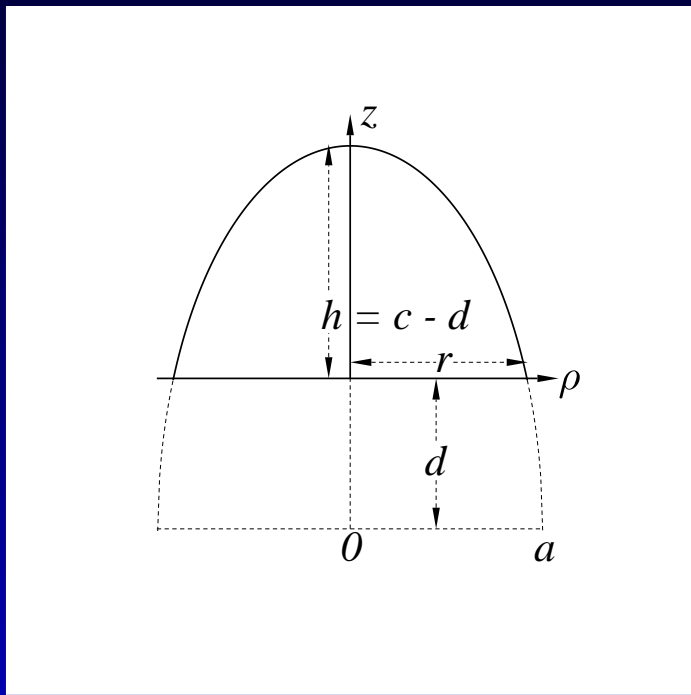
Contour plot E_{LDrel} , i = 0, 2



SHORT AND LONG SPHEROIDAL CAPS

Short Spheroidal Cap, $h < c$

Shape independent variables: δ , d_0



$$\rho^2 = \begin{cases} (a/c)^2(c^2 - z^2) & z \geq d \\ 0 & z < d \end{cases}$$

lengths in units of

$$R_s = 4^{1/3} r_s N^{1/3} [h_0^2(3 - h_0)]^{-1/3}$$

given $d_0 = d(\delta = 0)$

$$h_0 = 1 - d_0$$

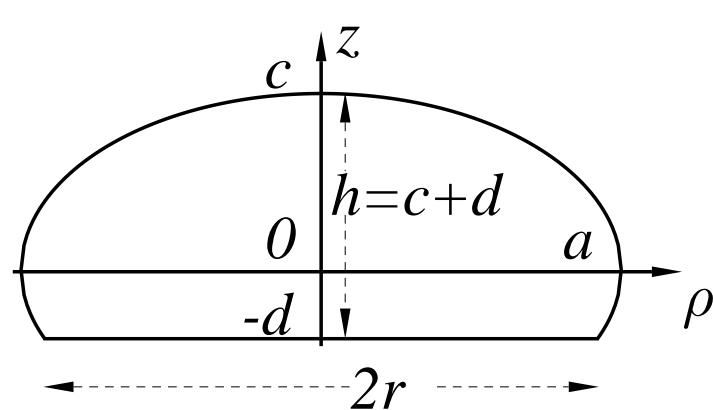
$$r_0 = \sqrt{1 - d_0^2}$$

$r^2 = (a/c)^2(c^2 - d^2)$ Volume conservation leads to

$$h^3 - 3ch^2 + c^3h_0^2(3 - h_0) = 0 \text{ with a real solution } h = ch_0$$

see also V.V. Semenikhina, A.G. Lyalin, A.V. Solov'yov, W. Greiner, J.E.T.P. 106 (2008) 679.

Long Spheroidal Cap, $h > c$



$$\rho^2 = \begin{cases} (a/c)^2(c^2 - z^2) & z \geq -d \\ 0 & z < -d \end{cases}$$

lengths in units of $R_s = 4^{1/3}r_sN^{1/3}[h_0^2(3 - h_0)]^{-1/3}$

given $d_0 = d(\delta = 0)$, $h_0 = 1 + d_0$, $r_0 = \sqrt{1 - d_0^2}$

$$r^2 = (a/c)^2(c^2 - d^2) \quad h = ch_0$$

Spherical cap, $\delta = 0$, various i

$$E_s^{sc0} = \frac{2h_0 + ir_0^2}{4} \left(\frac{R_s}{R_0} \right)^2 E_s^0 = \frac{2h_0 + ir_0^2}{4} \left(\frac{R_s}{R_0} \right)^2 4\pi R_0^2 \sigma$$

$$E_c^{sc0} = \frac{h_0 R_s}{2R_0} E_{curv}^0 = \frac{h_0 R_s}{2R_0} 4\pi R_0 \gamma_c$$

Deformation energy relative to the spherical cap

$$E^{sc} - E^{sc0} = E_s^{sc0} (B_{surf}^{sc} - 1) + E_c^{sc0} (B_{curv}^{sc} - 1)$$

Analytical relationships, short cap

Oblate shape ($a > c$, $e^2 = a^2/c^2 - 1$)

$$B_{surf}^{sc} = \frac{1}{ir_0^2 + 2h_0} \left[ir^2 + a \left(a - \frac{d}{c} \sqrt{c^2 + d^2 e^2} + \frac{c}{e} \ln \frac{a + ec}{ed + \sqrt{c^2 + d^2 e^2}} \right) \right]$$

$$B_{curv}^{sc} = \frac{h}{2h_0} + \frac{a^2}{2ec} (\arctan e - \arctan \frac{de}{c})$$

Prolate shape ($c > a$, $e^2 c^2 = c^2 - a^2$)

$$B_{surf}^{sc} = \frac{1}{ir_0^2 + 2h_0} \left\{ ir^2 + a \left[a - \frac{d}{c} \sqrt{c^2 - d^2 e^2} + \frac{c}{e} \left(\arcsin e - \arcsin \frac{de}{c} \right) \right] \right\}$$

$$B_{curv}^{sc} = \frac{h}{2h_0} + \frac{a^2}{4ec} \left(\ln \left| \frac{1+e}{1-e} \right| + \ln \left| \frac{ed-c}{ed+c} \right| \right)$$

Analytical relationships, long cap

Oblate shape ($a > c$, $e^2 = a^2/c^2 - 1$)

$$B_{surf}^{sc} = \frac{1}{ir_0^2 + 2h_0} \left[ir^2 + a \left(a + \frac{d}{c} \sqrt{c^2 + d^2 e^2} + \frac{c}{e} \ln \frac{a + ec}{\sqrt{c^2 + d^2 e^2} - ed} \right) \right]$$

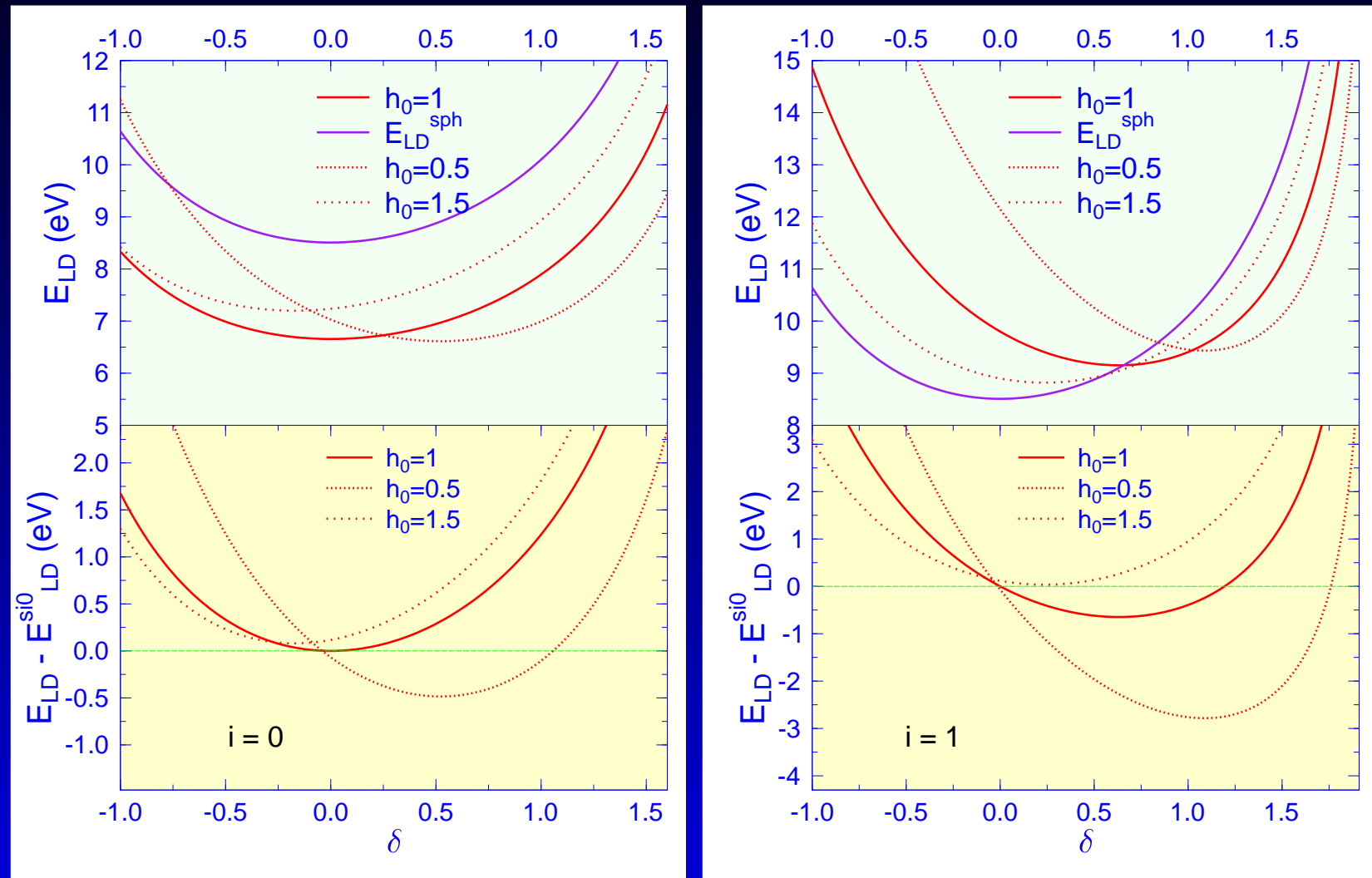
$$B_{curv}^{sc} = \frac{h}{2h_0} + \frac{a^2}{2ec} (\arctan e + \arctan \frac{de}{c})$$

Prolate shape ($c > a$, $e^2 c^2 = c^2 - a^2$)

$$B_{surf}^{sc} = \frac{1}{ir_0^2 + 2h_0} \left\{ ir^2 + a \left[a + \frac{d}{c} \sqrt{c^2 - d^2 e^2} + \frac{c}{e} \left(\arcsin e + \arcsin \frac{de}{c} \right) \right] \right\}$$

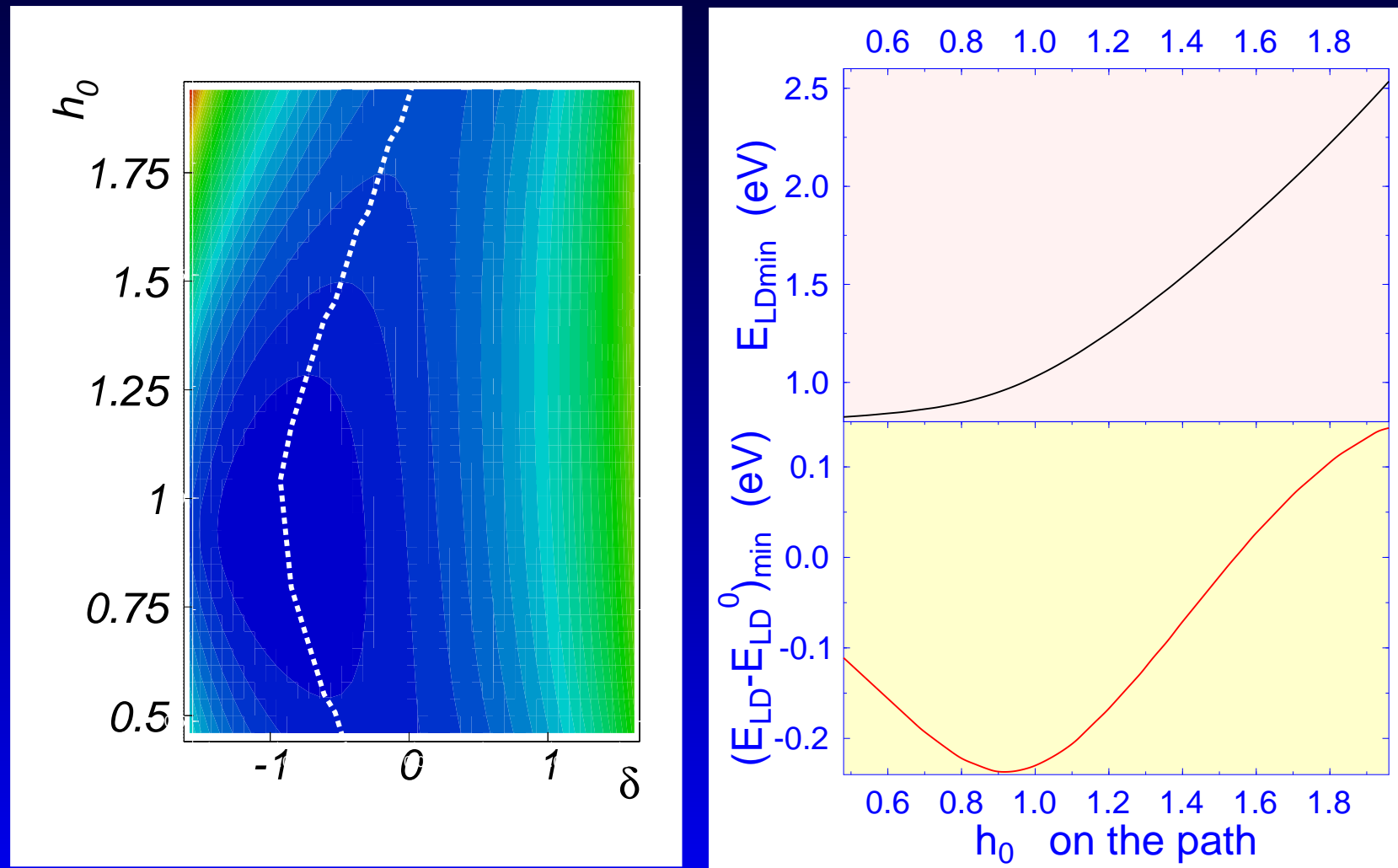
$$B_{curv}^{sc} = \frac{h}{2h_0} + \frac{a^2}{4ec} \left(\ln \left| \frac{1+e}{1-e} \right| + \ln \left| \frac{ed+c}{ed-c} \right| \right)$$

Deformation energy Na_{56} $i = 0, 1$

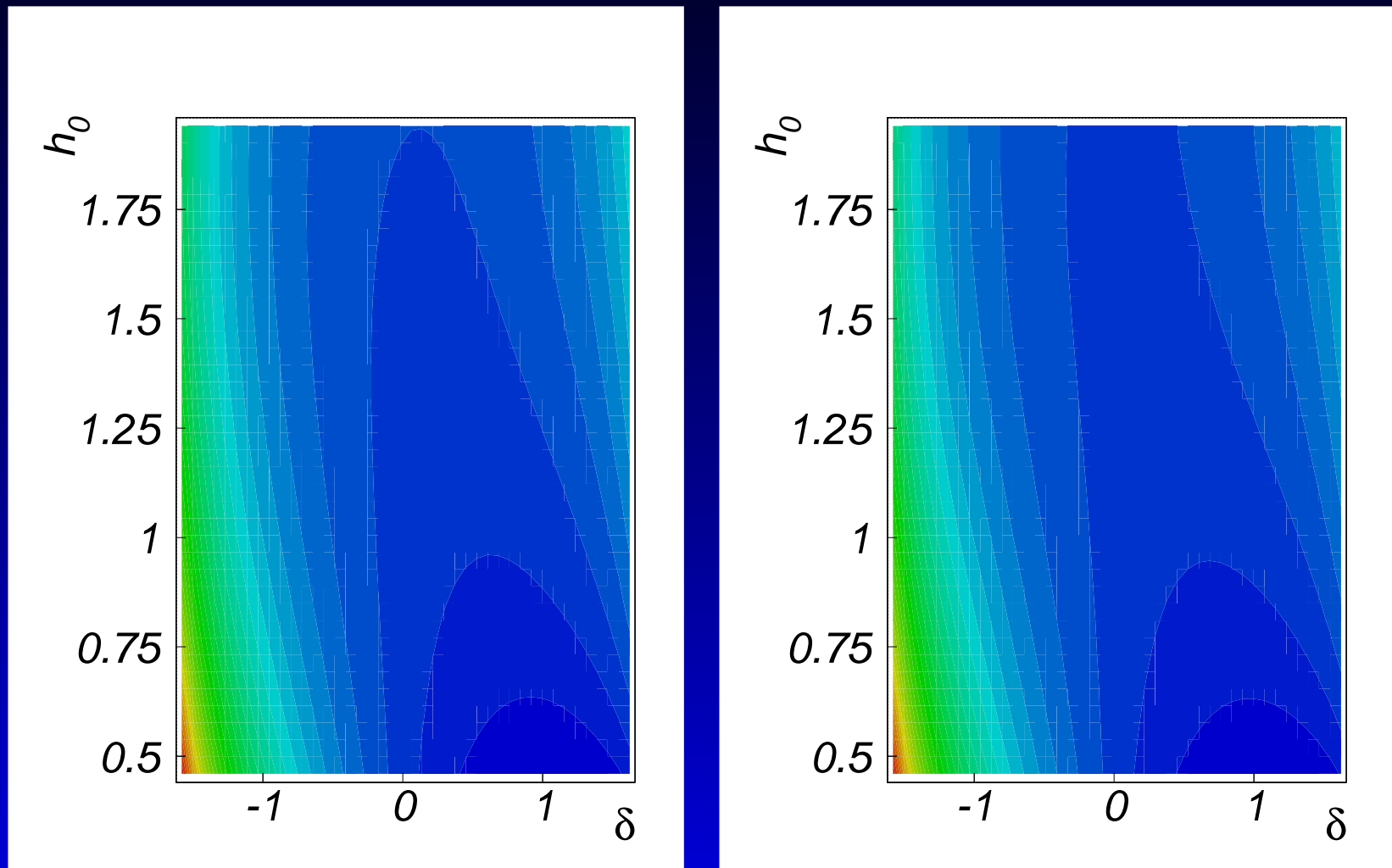


Contour plot E_{LDrel} , Na₈, $i = -0.76$

$(\delta, h_0)_{min} = -0.96, 0.92 ; E_{LDrel} = -0.237 ; E_{LDabs} = 0.964 \text{ eV}$

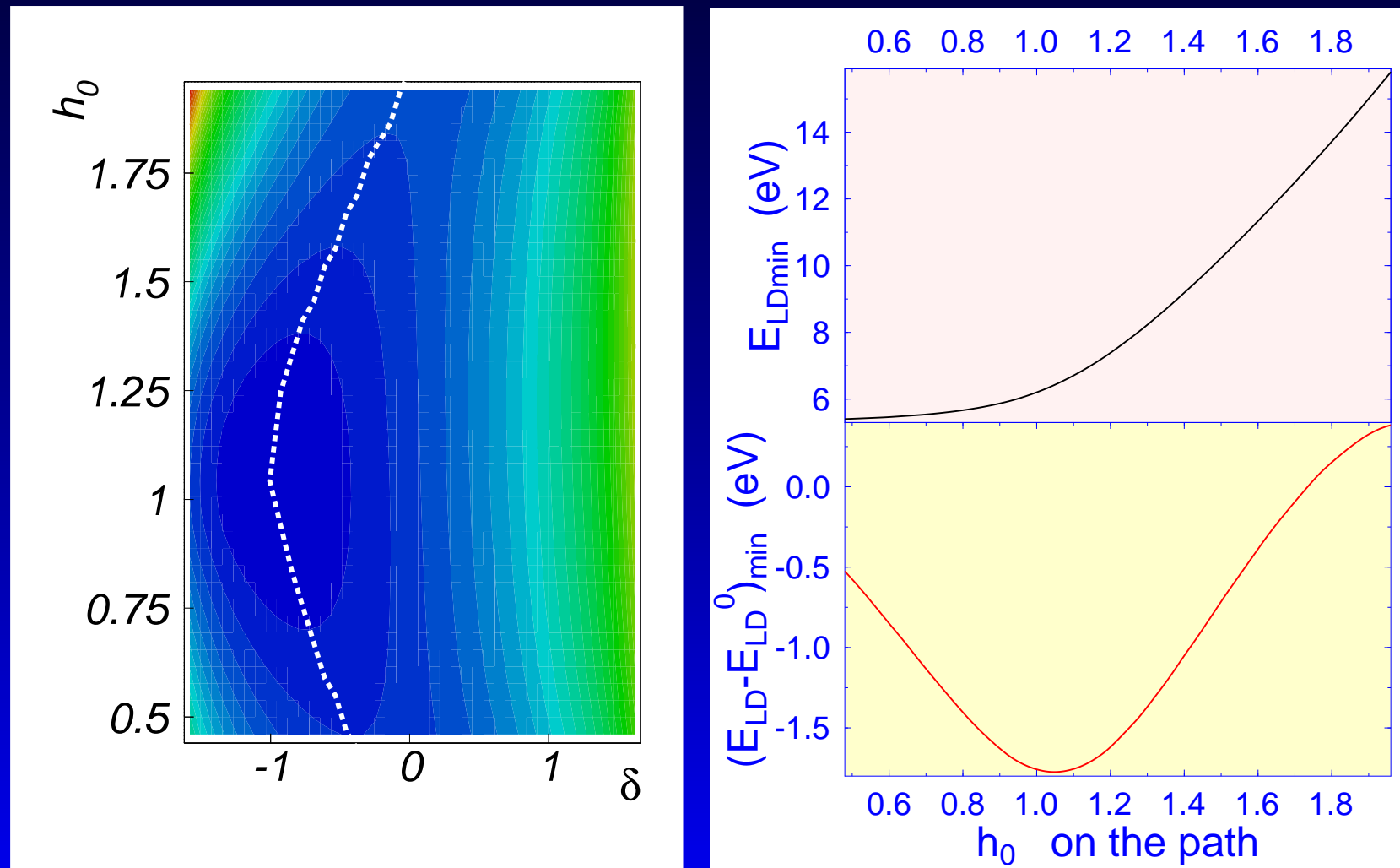


Contour pl E_{LDrel} $\mathbf{Na}_8, \mathbf{Na}_{148}$ $i = 1$



Contour plot E_{LDrel} Na₁₄₈ $i = -0.76$

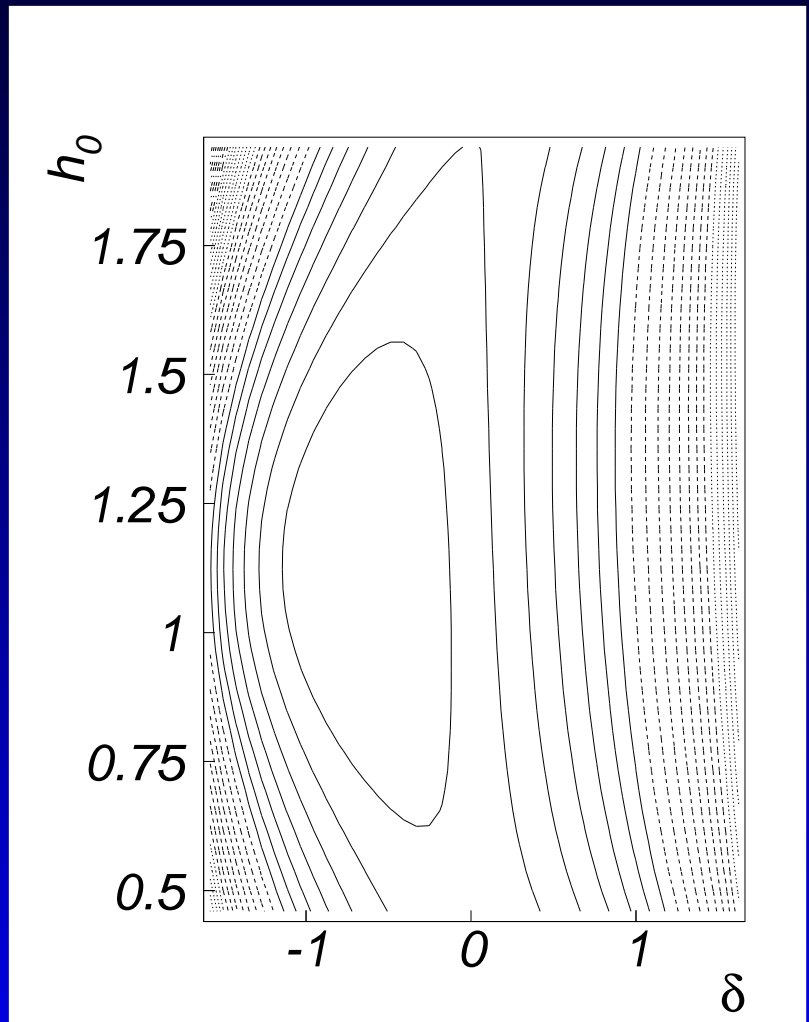
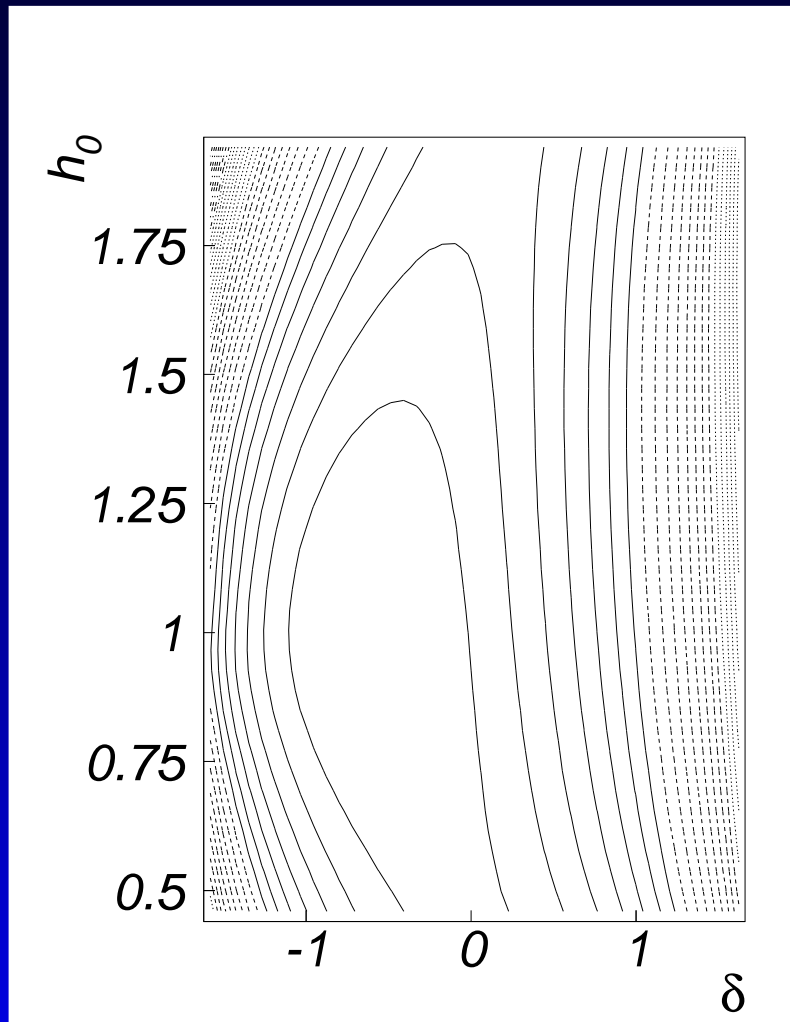
$(\delta, h_0)_{min} = -1.02, 1.05 ; E_{LDrel} = -1.778 ; E_{LDabs} = 6.429 \text{ eV}$



Contour pl E_{LDrel} $\mathbf{Na}_8, \mathbf{Na}_{148}$ $i = -0.58$

$(\delta, h_0)_{min} = -0.64, 0.98, \quad N=8$

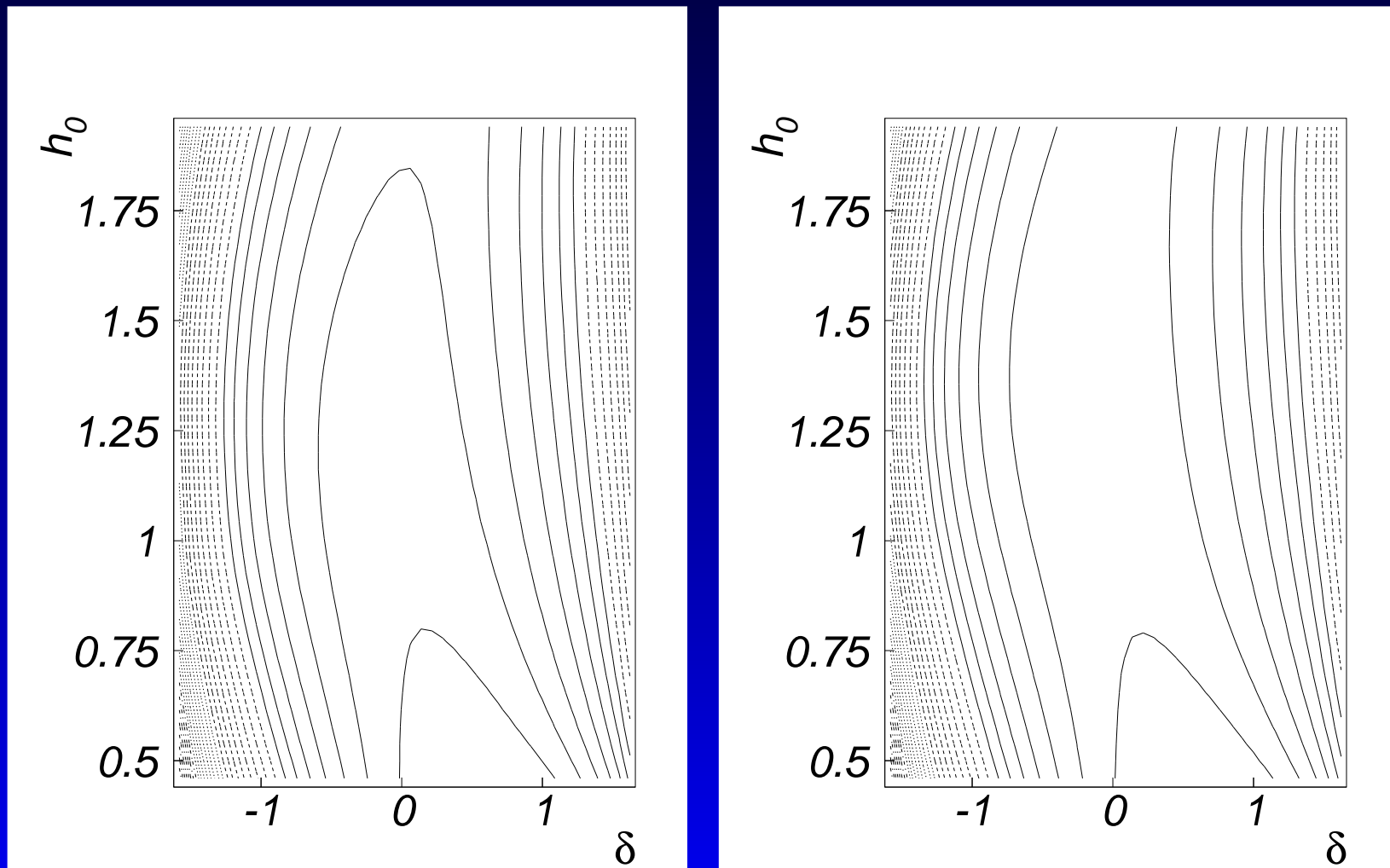
$-0.74, 1.12, \quad N=148$



Contour pl E_{LDrel} $\mathbf{Na}_8, \mathbf{Na}_{148}$ $i = 0$

$N = 8$: Min. at 0.54, 0.44. Max. at 0.06, 1.96

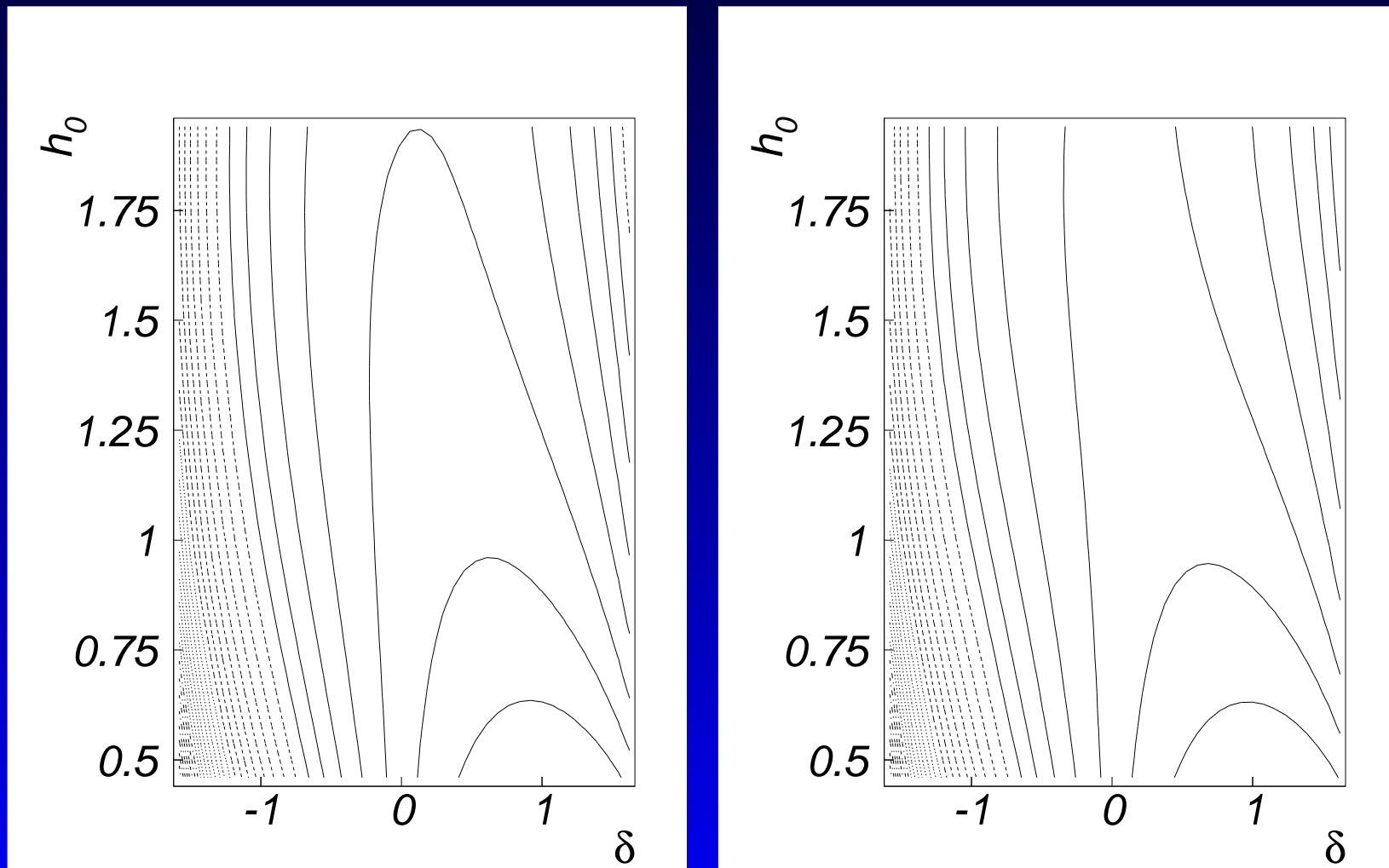
$N = 148$: Min. at 0.62, 0.44. Max. at -0.02, 1.96



Contour pl E_{LDrel} $\mathbf{Na}_8, \mathbf{Na}_{148}$ $i = 1$

$N = 8$: Min. at 1.1, 0.44. Max. at 0.14, 1.96

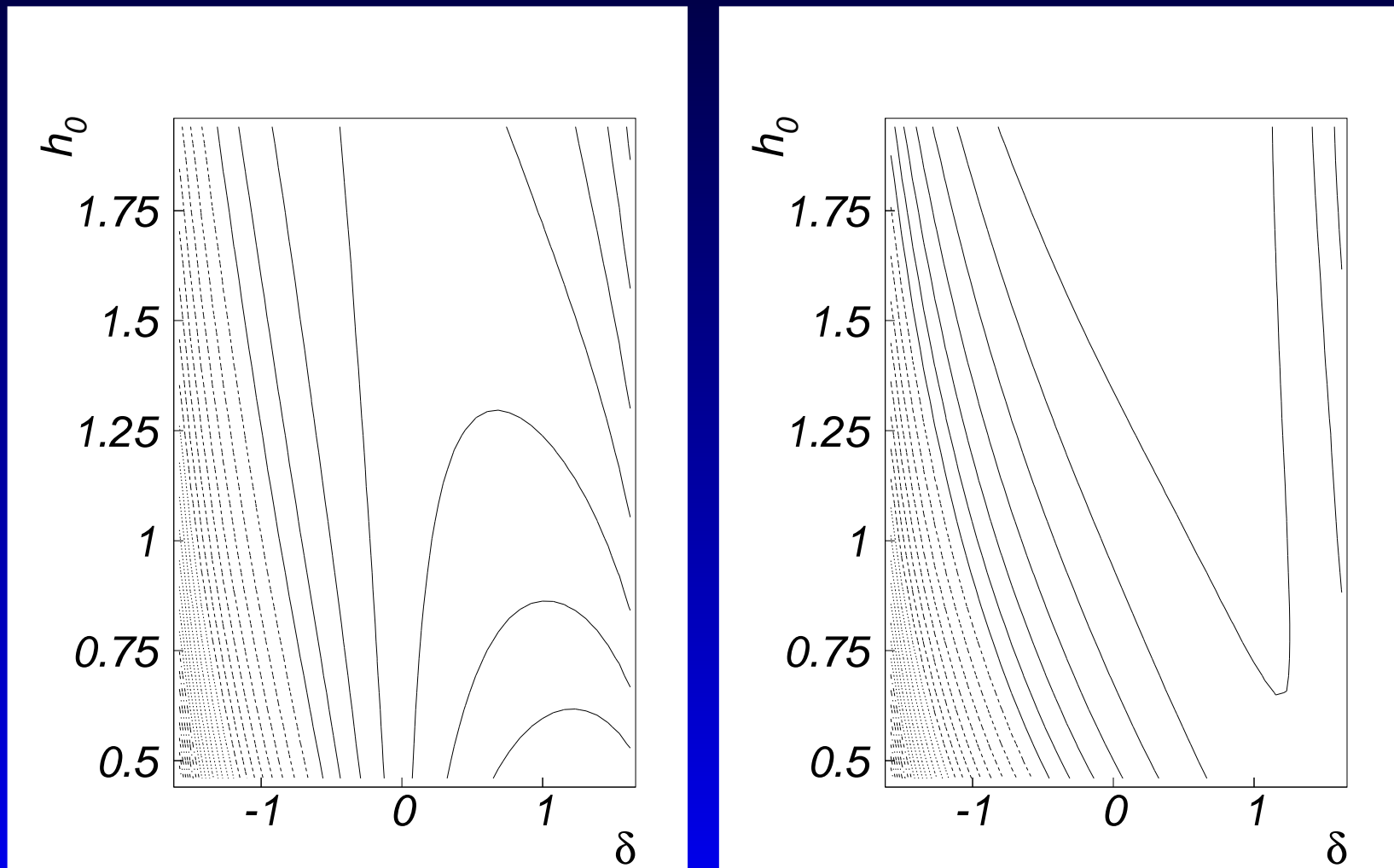
$N = 148$: Min. at 1.18, 0.44. Max. at 0.06, 1.96



Contour pl E_{LDrel} $\mathbf{Na}_8, \mathbf{Na}_{148}$ $i = 2$

$N = 8$: Min. at 1.34, 0.44. Max. at 0.14, 1.96

$N = 148$: Min. at 1.42, 0.44. Max. at 0.06, 1.96



Equilibrium shapes

Equil. shapes of short oblate spheroidal caps ($i < 0$) are less deformed than of long oblate spheroidal caps with the same h_0 . On the contrary for prolate shapes ($i \geq 0$).

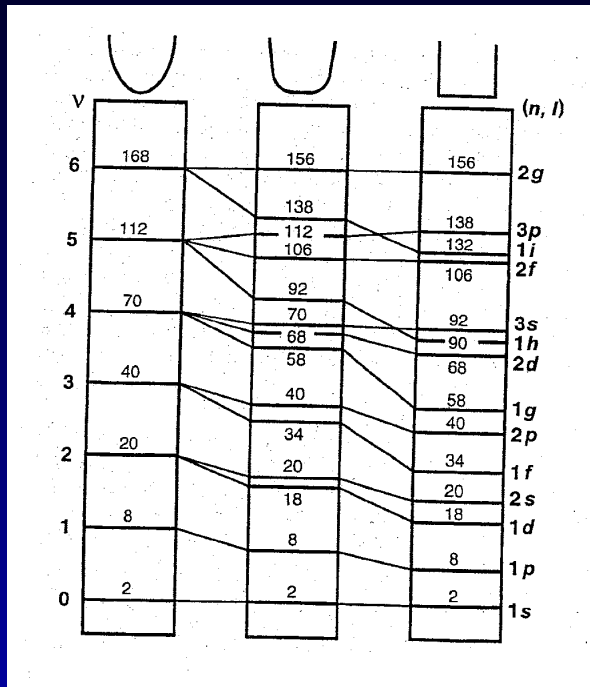
i	δ for $h_0 = 0.5$	δ for $h_0 = 1$	δ for $h_0 = 1.5$
	short cap	hemispheroid	long cap
-0.76	-0.53	-1.00	-0.62
-0.58	-0.16	-0.67	-0.50
0.00	0.52	0.00	-0.18
1.00	1.09	0.63	0.24
2.00	1.36	0.97	0.52

For $i < 0$ the minimum deformation energy occurs around $h_0 = 1$ (hemispheroidal shape)

DEFORMED SINGLE PARTICLE SPHEROIDAL SHELL MODEL

In a small metallic cluster the conduction electrons are confined. Consequently their quantum energy level spectrum is discrete, in contrast to the continuous spectrum of the infinite bulk.

Spherical shell model



letter	name	l
s	sharp	0
p	principal	1
d	diffuse	2
f	fundamental	3
g		4
h		5
etc		

Spectroscopic notation of clusters follows that of nuclei. The letters s, p, d, ... are associated to angular momentum \mathbf{l} .

The spectrum depends on the well shape. High \mathbf{l} states probe mainly the outer regions of the potential (centrifugal effects). The sensitivity to the details of the potential is greatest for higher energy electrons, because the electronic wavelengts are smaller for those energy levels.

Jahn-Teller effect (studied for nuclei by Nilsson): for open shell clusters (which are degenerate in their spherical state), the total energy can be lowered by distorting the cluster (lifting the degeneracy).

Spheroidal harmonic oscillator I

The harmonic oscillator (HO) potential part of the Clemenger-Nilsson model (**K.L. Clemenger, Phys. Rev. B 32 (1985) 1359**)

$$V = \frac{MR_0^2}{2}(\omega_{\perp}^2\rho^2 + \omega_z^2z^2) = \frac{M\omega_0^2R_0^2}{2} \left[\rho^2 \left(\frac{2+\delta}{2-\delta} \right)^{2/3} + z^2 \left(\frac{2-\delta}{2+\delta} \right)^{4/3} \right]$$

The eigenvalues of the 3-dimensional Hamiltonian are

$$E = \hbar\omega_{\perp}(n_{\perp} + 1) + \hbar\omega_z \left(n_z + \frac{1}{2} \right)$$

The main quantum number $n = n_{\perp} + n_z$. In units of $\hbar\omega_0$

$$\epsilon = \frac{E}{\hbar\omega_0} = \frac{2}{(2-\delta)^{1/3}(2+\delta)^{2/3}} \left[n + \frac{3}{2} + \delta \left(n_{\perp} - \frac{n}{2} + \frac{1}{4} \right) \right]$$

Spheroidal HO II

The single-particle shell gap (K.L. Clemenger, 1985):

$$\hbar\omega_0 = \frac{49 \text{ eV bohr}^2}{r_s^2 N^{1/3}} \left[1 + \frac{t}{r_s N^{1/3}} \right]^{-2} = \frac{13.72 \text{ eV \AA}^2}{r_s R_0} \left[1 + \frac{t}{r_s N^{1/3}} \right]^{-2}$$

r_s is the Wigner-Seitz radius (atomic units), t is the electronic spillout of the neutral cluster (we assume $t = 0$).

Levels are labeled by two quantum numbers (n, n_{\perp}) — integers. For every $n = 0, 1, 2, \dots$ one has $n_{\perp} = 0, 1, 2, \dots, n$. Each level may accommodate $2n_{\perp} + 2$ particles. One has $(n + 1)(n + 2)$ atoms in a completely filled shell. The magic numbers for spherical shapes ($\delta = 0$) are $(n + 1)(n + 2)(n + 3)/3 = 2, 8, 20, 40, 70, 112, 168\dots$

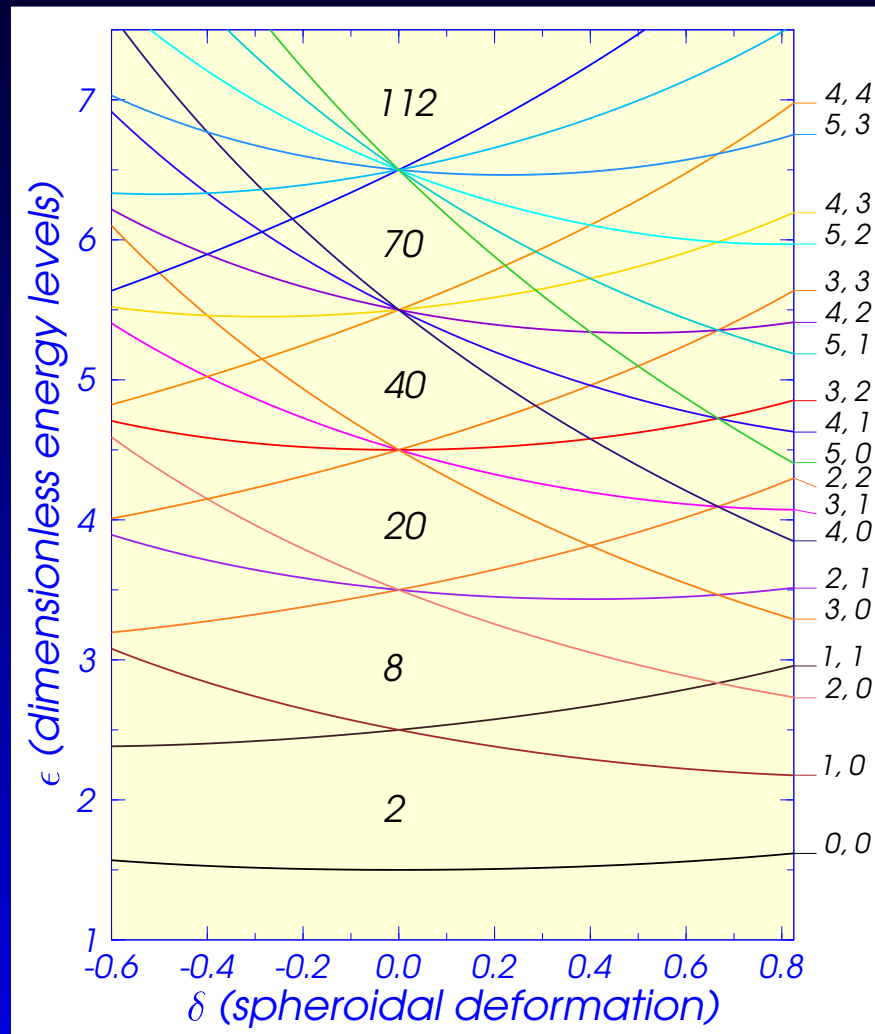
Spheroidal HO energy levels

Label: n, n_{\perp} .

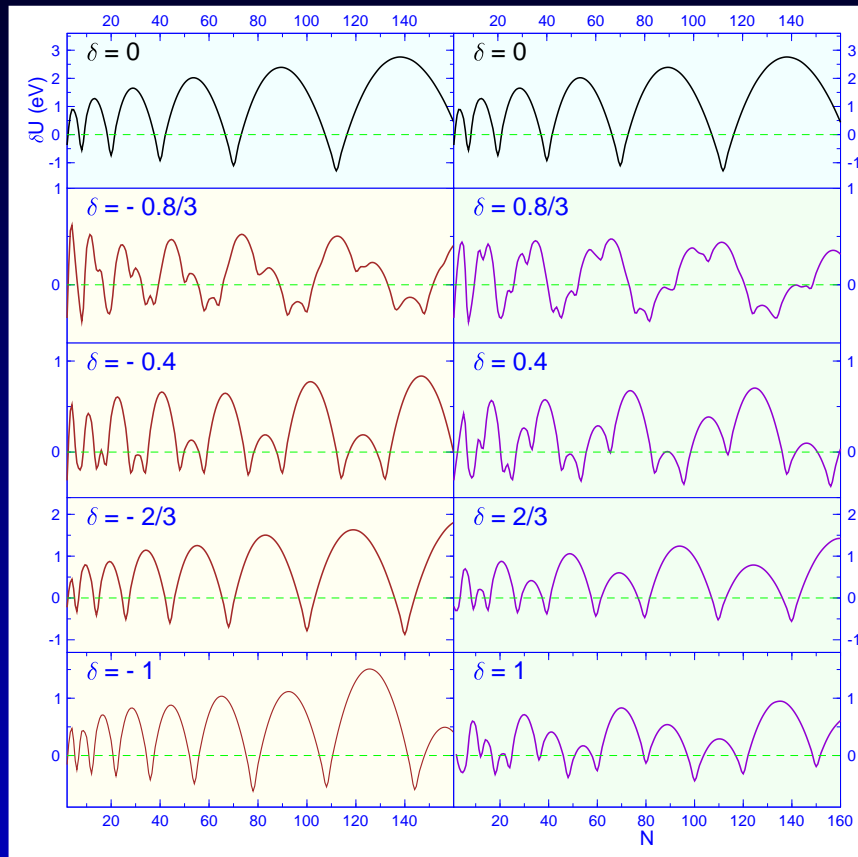
For $\delta > 0$ (prolate shape) at $n_{\perp} = 0$ the energy decreases with deformation, except for $n = 0$, $\epsilon(n_{\perp} = 0) = [2n+3-\delta(n-1/2)]/[(2-\delta)^{1/3}(2+\delta)^{2/3}]$

When $n_{\perp} = n$ it increases $\epsilon(n_{\perp} = n) = [2n+3+\delta(n+1/2)]/[(2-\delta)^{1/3}(2+\delta)^{2/3}]$

Remark a 2nd degeneracy at $\delta = 2/3$



Magic numbers of spheroidal HO



The spherical magic numbers

$(n + 1)(n + 2)(n + 3)/3$ are
2, 8, 20, 40, 70, 112, 168 ...

The magic numbers at the oblate spheroidal superdeformed shape ($\delta = -2/3$) are: 2, 6, 14, 26, 44, 68, 100, 140, ...

Magic numbers of spheroidal HO II

Sphere ($\delta = 0$): 2, 8, 20, 40, 70, 112, 168 ...

Oblate shapes:

$\delta = -0.8/3$ 2, 8, 18, 20, 34, 38, 58, 64, 92, 100, 136, 148,

$\delta = -0.4$ 2, 6, 8, 14, 18, 28, 34, 48, 58, 76, 90, 114, 132,

$\delta = -2/3$ 2, 6, 14, 26, 44, 68, 100, 140,

$\delta = -1$ 2, 6, 12, 22, 36, 54, 78, 108, 144,

Prolate shapes:

$\delta = 0.8/3$ 2, 8, 20, 22, 42, 46, 76, 82, 124, 134,

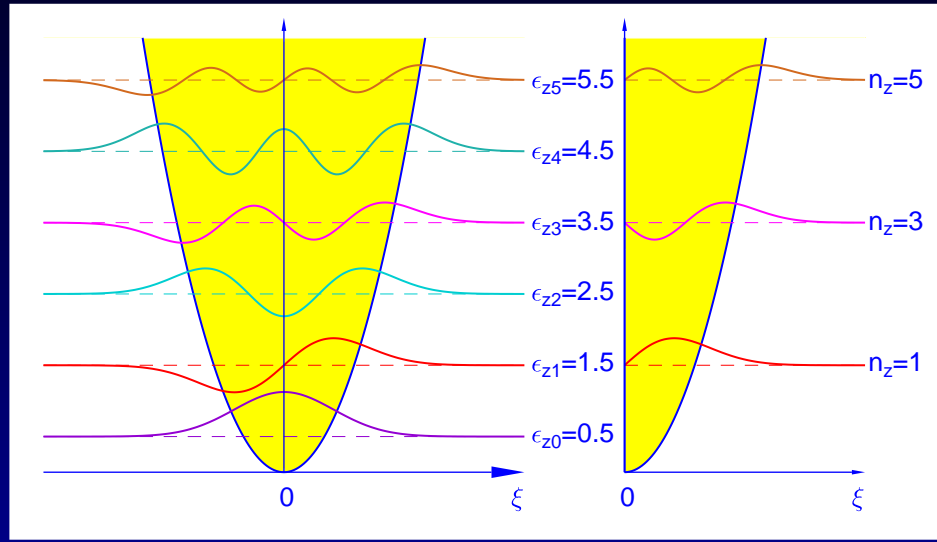
$\delta = 0.4$ 2, 8, 10, 22, 26, 46, 54, 66, 84, 96, 114, 138, 156,

$\delta = 2/3$ 2, 4, 10, 16, 28, 40, 60, 80, 110, 140,

$\delta = 1$ 4, 12, 18, 24, 36, 48, 60, 80, 100, 120, 150,

DEFORMED SINGLE PARTICLE HEMISPHEROIDAL SHELL MODEL

New (hemispheroidal) HO



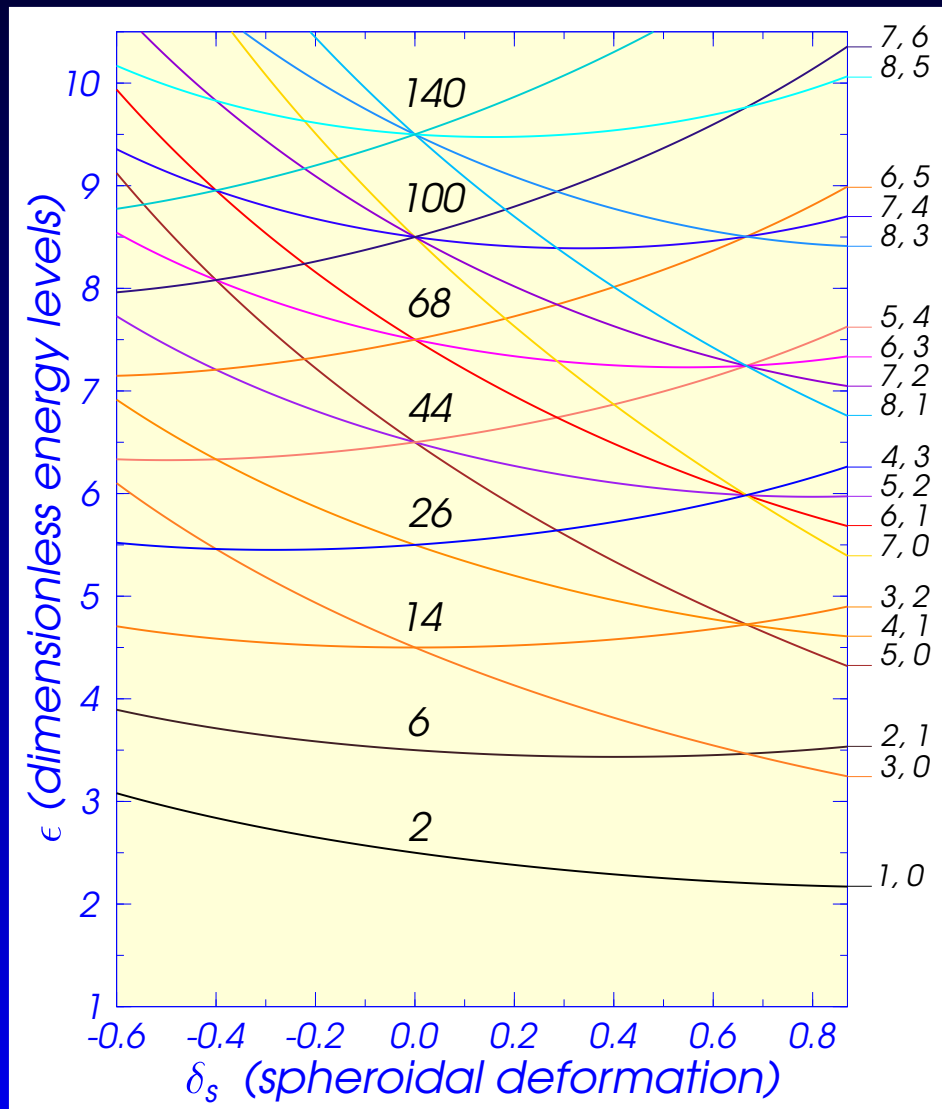
Axially-symmetric 3dim
HO $H\Psi = E\Psi$
 $H = T + V_\rho(\rho) + V_z(z)$
 $\Psi = \psi_{n_r}^m(\eta)\Phi_m(\varphi)Z_{n_z}(\xi)$
 $E_n = \hbar\omega_\perp(n_\perp + 1) + \hbar\omega_z(n_z + 1/2)$

The main quantum number $n = n_\perp + n_z = 0, 1, 2, 3, \dots n$

$$Z_{n_z}(\xi) = N_{n_z} e^{-\xi^2/2} H_{n_z}(\xi) \quad \xi = zR_0/\sqrt{\hbar/M\omega_z} \text{ - dim.less}$$

N_{n_z} - ortonorm.constant Hermite polynomials with parity $(-1)^{n_z}$ meaning $H_{2n_z}(-\xi) = H_{2n_z}(\xi)$ and $H_{2n_z+1}(-\xi) = -H_{2n_z+1}(\xi)$. For hemispheroidal HO $V_z(0) \rightarrow \infty$. One should have $Z_{n_z}(\xi = 0) = 0$. **Only odd n_z values remain.**

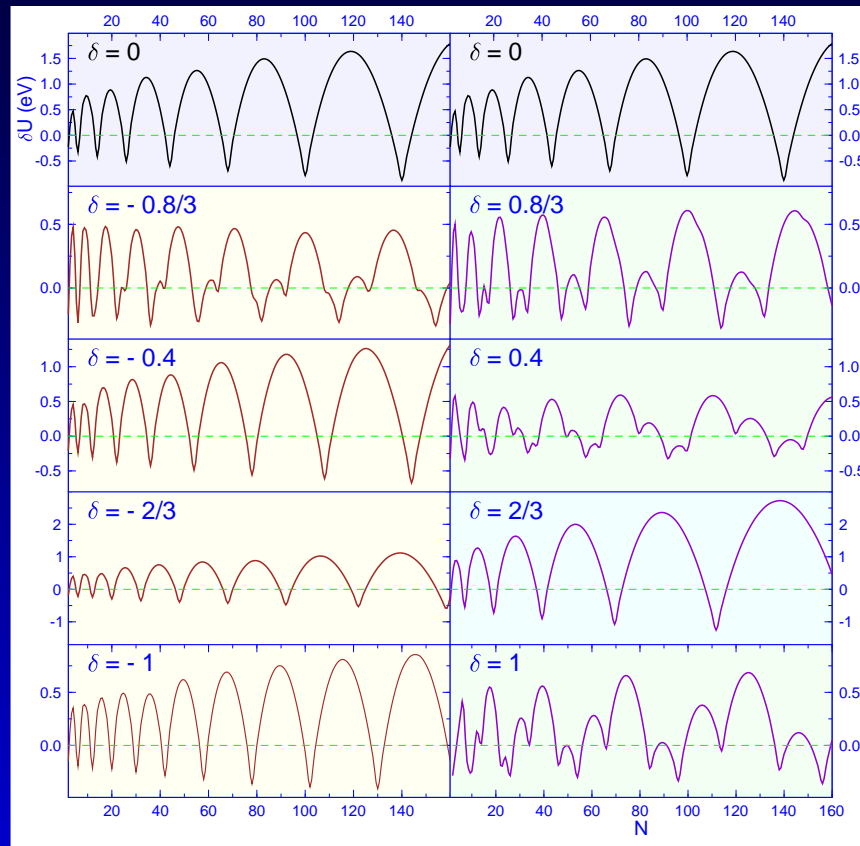
Hemispheroidal HO en. levels



At every pair (n, n_{\perp}) , labeling an energy level, only those values are acceptable which lead to $n_z = n - n_{\perp} \geq 1$ — odd numbers.

The hemispherical magic numbers are equal to those obtained at the oblate spheroidal superdeformed shape, $\delta = -2/3$ i.e. 2, 6, 14, 26, 44, 68, 100, 140, ...

Magic numbers of hemispher. HO



The contrib. to the hemispherical magic numbers of shells with:

- (1) odd n : $(n + 1)^2/2$,
- (2) even n : $n(n + 2)/2$.

Semi-spherical m.n. are identical to those obtained at the oblate spheroidal superdeformed shape ($\delta = -2/3$: 2, 6, 14, 26, 44, 68, 100, 140, ...)

Magic numbers of hemisph. HO II

Semi-sphere ($\delta = 0$): 2, 6, 14, 26, 44, 68, 100, 140, ...

Oblate hemispheroidal shapes:

$\delta = -0.8/3$ 2, 6, 12, 22, 26, 36, 42, 56, 64, 82, 92, 114, 126, 154,

$\delta = -0.4$ 2, 6, 12, 22, 36, 54, 78, 108, 144,

$\delta = -2/3$ 2, 6, 12, 20, 32, 48, 68, 92, 122, 158,

$\delta = -1$ 2, 6, 20, 30, 42, 58, 78, 102, 130,

Prolate hemispheroidal shapes:

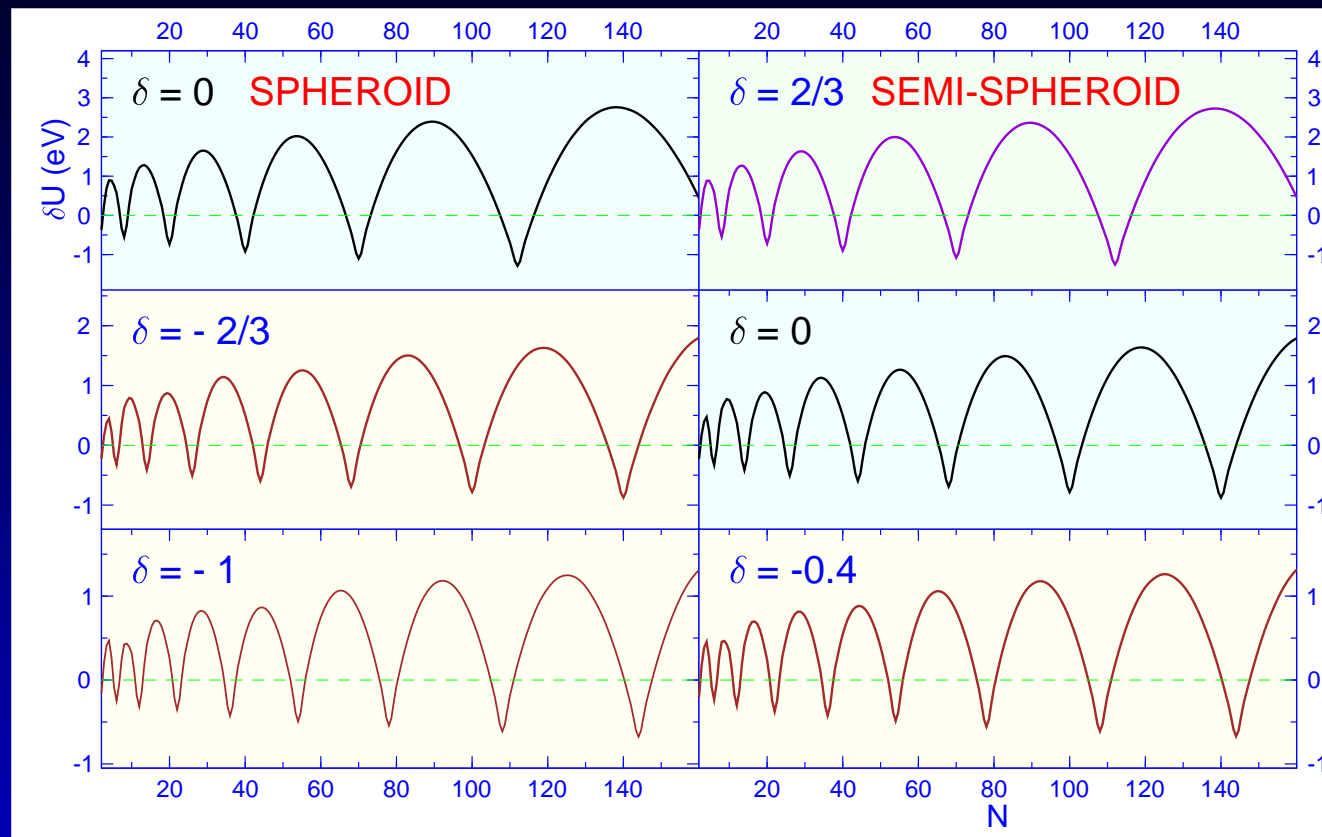
$\delta = 0.8/3$ 2, 6, 8, 14, 18, 28, 34, 48, 58, 76, 90, 114, 132,

$\delta = 0.4$ 2, 8, 18, 20, 34, 38, 50, 58, 64, 80, 92, 100,

$\delta = 2/3$ 2, 8, 20, 40, 70, 112, 168,

$\delta = 1$ 2, 8, 10, 14, 22, 26, 46, 54, 66, 84, 96, 114, 138, 156,

Comparison of degeneracies



Striking: magic numbers at the prolate superdef. shape ($\delta = 2/3$)
are identical to those obtained at the spherical shape
 $(n + 1)(n + 2)(n + 3)/3 = 2, 8, 20, 40, 70, 112, 168 \dots$

Influence of \mathbf{l}^2 term (I)

$$H = -\frac{\hbar^2 \Delta}{2M} + V_{osc} - \hbar \omega_0 U (\mathbf{l}^2 - \langle \mathbf{l}^2 \rangle_n)$$

$$V_{osc} = \frac{M \omega_0^2 R_0^2}{2} \left(\frac{\rho^2}{a^2} + \frac{z^2}{c^2} \right) \quad U = 0.04 \text{ and } \langle \mathbf{l}^2 \rangle_n = n(n+3)/2$$
$$\mathbf{l} = \nabla \mathbf{V}_{osc} \times \hat{\mathbf{p}} \quad \mathbf{l}^2 = 0.5(\mathbf{l}^+ \mathbf{l}^- + \mathbf{l}^- \mathbf{l}^+) + l_z^2$$

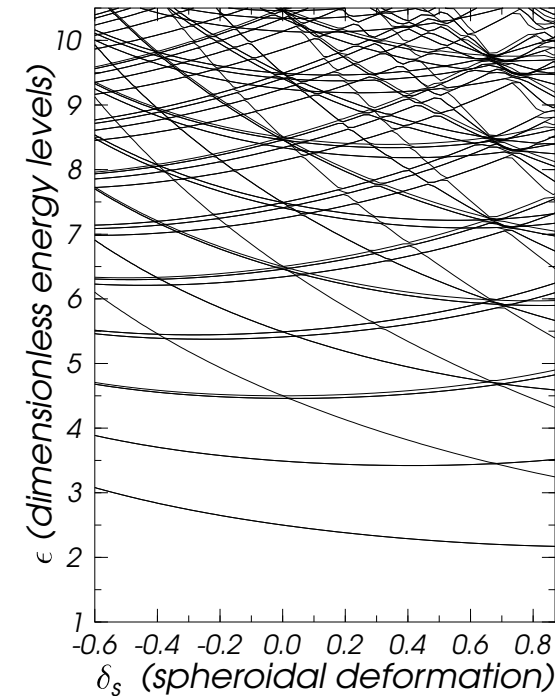
$$\epsilon_n = \frac{E_n}{\hbar \omega_0} = \frac{n_\perp + 1}{a} + \frac{n_z + 1/2}{c} - \frac{Um^2}{4a^4} + \frac{Un(n+3)}{2}$$

$$|m| = n_\perp - 2i \quad i = 0, 1, \dots (n_\perp - 1)/2 \text{ for odd } n_\perp \text{ or } (n_\perp - 2)/2 \text{ for even } n_\perp.$$

The possible nondiagonal terms coming from $(\hat{l}^+ \hat{l}^- + \hat{l}^- \hat{l}^+)/2$ are not present since their contribution vanishes (n_z odd).

$|m| = (n_\perp - 2i)$ with $i = 0, 1, \dots$ U — strength of interaction

Influence of \mathbf{l}^2 term (II)



For lower levels (say up to 10 closed shells), the sequence of the magic numbers at the maximum degeneracy, $\delta = 2/3$, remain the same: $N = 2, 8, 20, 40, 70, 112, 168$. At very large oblate deformations, leading to “pan-cake” shapes approximating a 2D situation, one of the **magic number is 6**, in agreement with the experiments of Chiu et al.

Ya-Ping Chiu *et al.*, Magic Numbers of Atoms in Surface-Supported Planar Clusters, *Phys. Rev. Lett.* **97** (2006) 165504.

MICROSCOPIC SHELL AND PAIRING CORRECTIONS

Shell corrections (I)

The average potential felt by one atom can be either of finite depth (e.g. Woods-Saxon) or of infinite depth (e.g. harmonic osc. potential, Clemenger-Nilsson potential, or the two-center shell model potential). We know the doubly degenerate discrete energy levels $\epsilon_i = E_i/\hbar\omega_0^0$ in units of $\hbar\omega_0^0 \approx (13.72 \text{ eV } \text{\AA}^2)/(r_s^2 N^{1/3})$, arranged in order of increasing energy.

The smoothed-level distribution density is obtained by averaging the actual distribution over a finite energy interval $\Gamma = \gamma\hbar\omega_0^0$, with $\gamma \simeq 1$,

$$\tilde{g}(\epsilon) = \left\{ \sum_{i=1}^{n_m} [2.1875 + y_i(y_i(1.75 - y_i/6) - 4.375)] e^{-y_i} \right\} (1.77245385\gamma)^{-1}$$

where $y = x^2 = [(\epsilon - \epsilon_i)/\gamma]^2$. The summation is performed up to the level n_m fulfilling the condition $|x_i| \geq 3$.

Shell corrections (II)

The Fermi energy, $\tilde{\lambda}$, of this distribution is given by

$$N = 2 \int_{-\infty}^{\tilde{\lambda}} \tilde{g}(\epsilon) d\epsilon$$

leading to a non-linear equation in $\tilde{\lambda}$, solved numerically.

The total energy of the uniform level distribution

$$\tilde{u} = \tilde{U}/\hbar\omega_0^0 = 2 \int_{-\infty}^{\tilde{\lambda}} \tilde{g}(\epsilon) \epsilon d\epsilon$$

In units of $\hbar\omega_0^0$ the shell corrections are calculated for each deformation δ

$$\delta u(n, \delta) = \sum_{i=1}^n 2\epsilon_i(\delta) - \tilde{u}(n, \delta)$$

$n = N/2$ particles.

Pairing corrections (I)

For atomic clusters there is no pairing force. We only consider pairing corrections for a technical reason: to obtain smoothed microscopic corrections.

Doubly degenerate levels $\{\epsilon_i\}$ in units of $\hbar\omega_0^0$. $N/2$ levels are occupied. n levels below & n' above Fermi energy contribute to pairing,

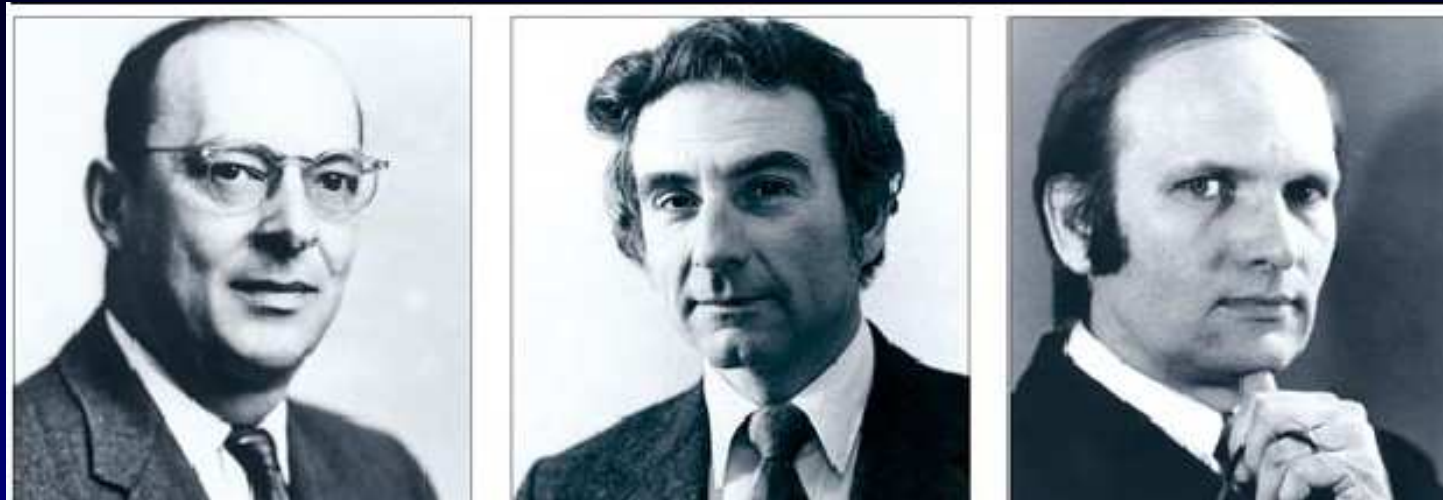
$n = n' = \Omega \tilde{g}_s / 2$. Cutoff energy, $\Omega \simeq 1 \gg \tilde{\Delta} = 1.3416 / (\sqrt{N} \hbar \omega_0^0)$

The gap Δ and Fermi energy λ are solutions of the BCS eqs:

$$0 = \sum_{k_i}^{k_f} \frac{\epsilon_k - \lambda}{\sqrt{(\epsilon_k - \lambda)^2 + \Delta^2}} ; \quad \frac{2}{G} = \sum_{k_i}^{k_f} \frac{1}{\sqrt{(\epsilon_k - \lambda)^2 + \Delta^2}}$$

$$k_i = Z/2 - n + 1, \quad k_f = Z/2 + n', \quad \frac{2}{G} \simeq 2\tilde{g}(\tilde{\lambda}) \ln \left(\frac{2\Omega}{\tilde{\Delta}} \right).$$

Bardeen, Cooper, Schrieffer



John Bardeen, Leon N. Cooper, John R. Schrieffer
Nobel Prize 1972: theory of superconductivity.

quasiparticle — a free particle (combination of a particle and its pairing interaction). The same spin ($1/2$) as the particle.

Cooper showed that an arbitrarily small attraction between electrons in a metal can cause a paired state of electrons to have a lower energy than the Fermi energy, which implies that the pair is bound. In normal superconductors, this attraction is due to the electron-phonon interaction. A *Cooper pair* is a boson. The tendency for all the Cooper pairs in a body to condense into the same ground state is responsible for the superconductivity.

Pairing corrections (II)

As a consequence of the pairing correlation, the levels below the Fermi energy are only partially filled, while those above the Fermi energy are partially empty. Occup. probab. by a quasiparticle (u_k) or hole (v_k)

$$v_k^2 = [1 - (\epsilon_k - \lambda)/E_k]/2; u_k^2 = 1 - v_k^2. \text{ Quasip. energy}$$

$$E_\nu = \sqrt{(\epsilon_\nu - \lambda)^2 + \Delta^2}.$$

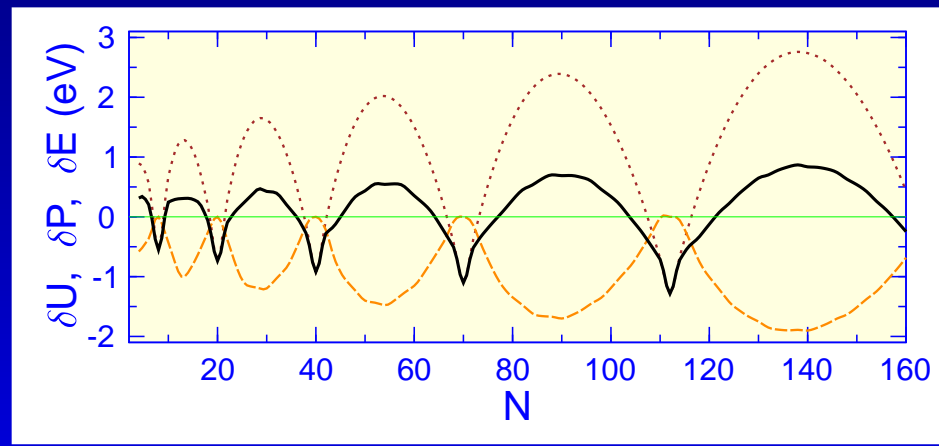
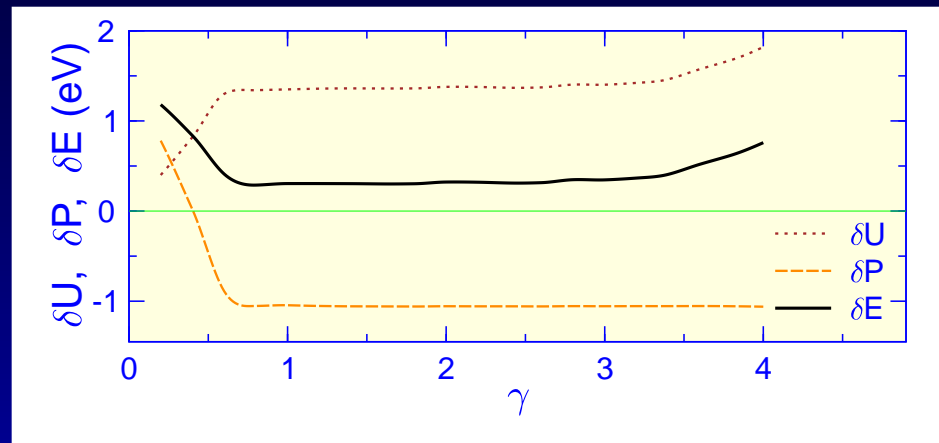
The pairing correction $\delta p = p - \tilde{p}$, represents the difference between the pairing correlation energies for the discrete level distribution

$$p = \sum_{k=k_i}^{k_f} 2v_k^2\epsilon_k - 2 \sum_{k=k_i}^{Z/2} \epsilon_k - \frac{\Delta^2}{G}$$
 and for the continuous level

distribution $\tilde{p} = -(\tilde{g}\tilde{\Delta}^2)/2 = -(\tilde{g}_s\tilde{\Delta}^2)/4$. Compared to shell correction, the pairing correction is out of phase and smaller, hence it has a smoothing effect.

Shell and pairing corrections

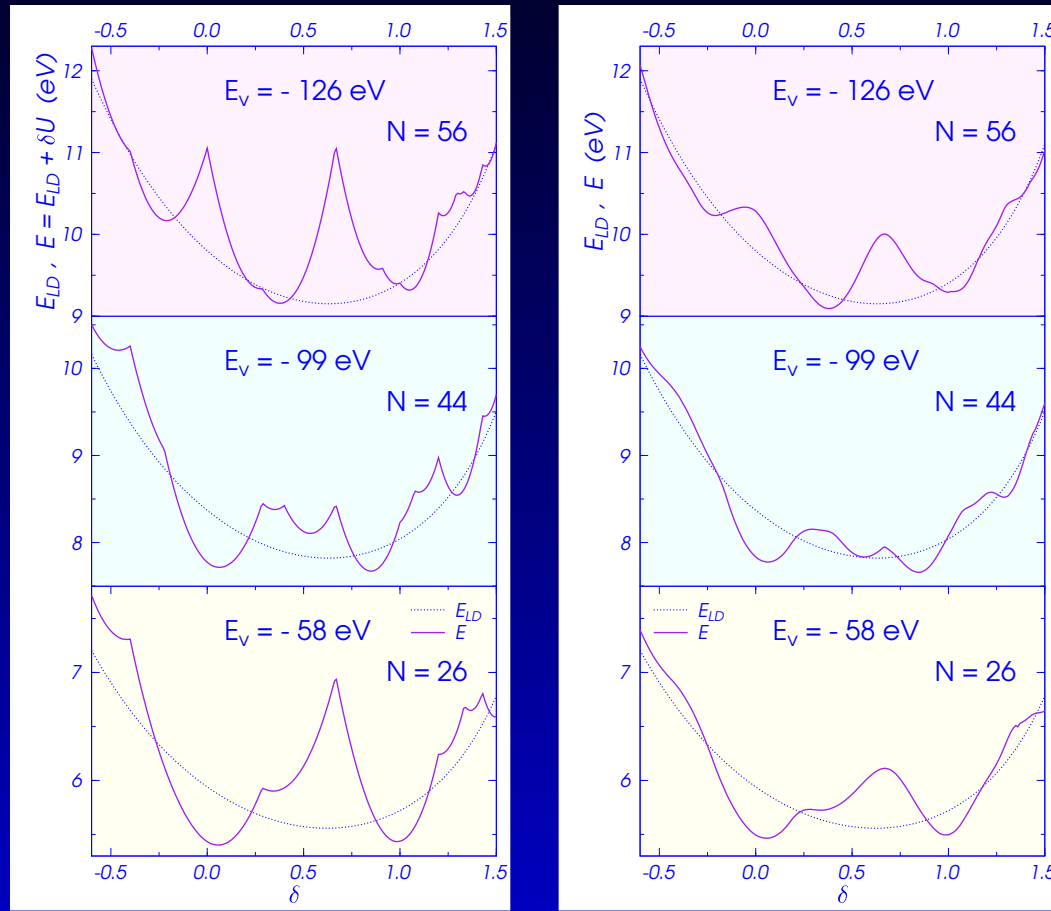
Plateau condition for $N = 90$, $\delta = -2/3$. We choose
 $\gamma = 1.2$



Variation with N for $\delta = 0$. HO magic numbers: $(n+1)(n+2)(n+3)/3 = 2, 8, 20, 40, 70, 112, 168, \dots$

RESULTS OF MACROSCOPIC- MICROSCOPIC CALCULATIONS FOR HEMISPEROIDAL CLUSTERS

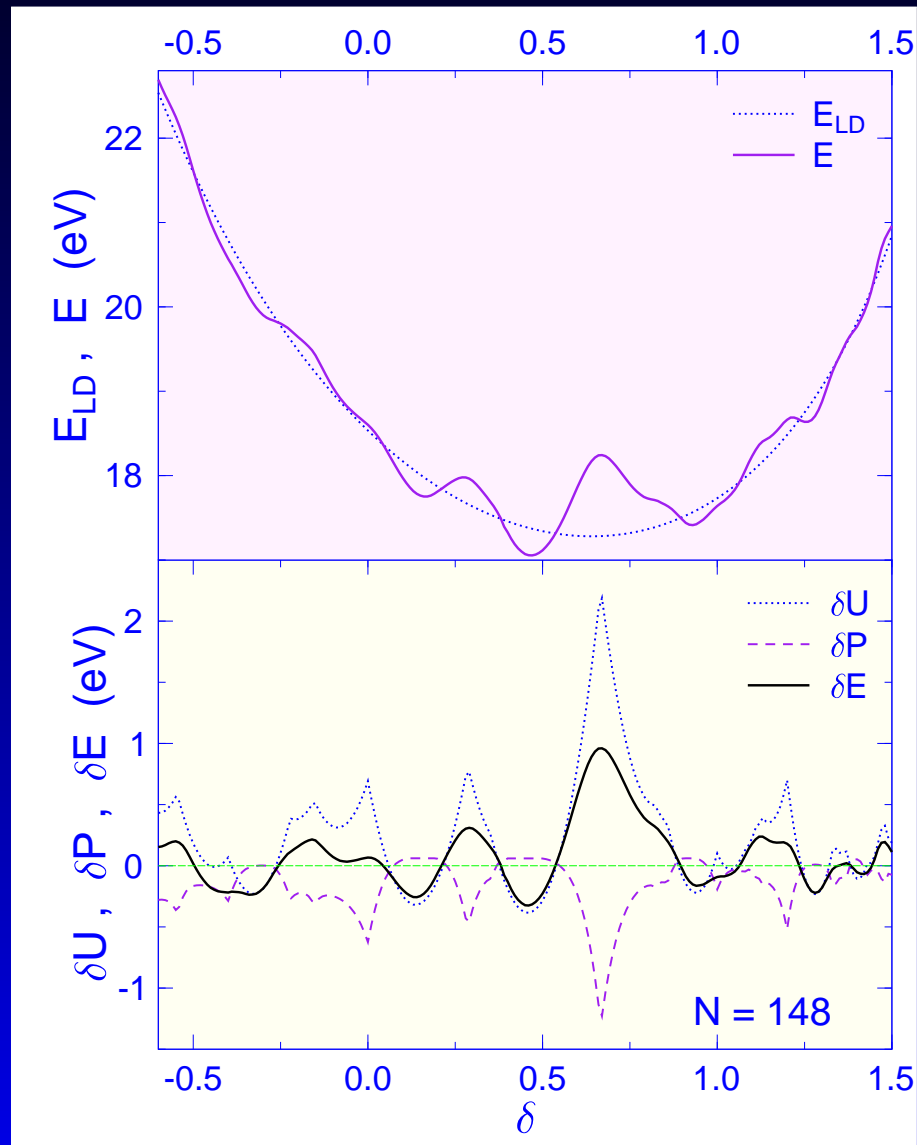
M-MA: hemisph. Na clusters



Ground state deformations:
 $\delta = 0.04$ for Na_{26}
 $\delta = 0.84$ for Na_{44} despite it is a closed shell cluster
 $\delta = 0.38$ for the mid-shell Na_{56} cluster

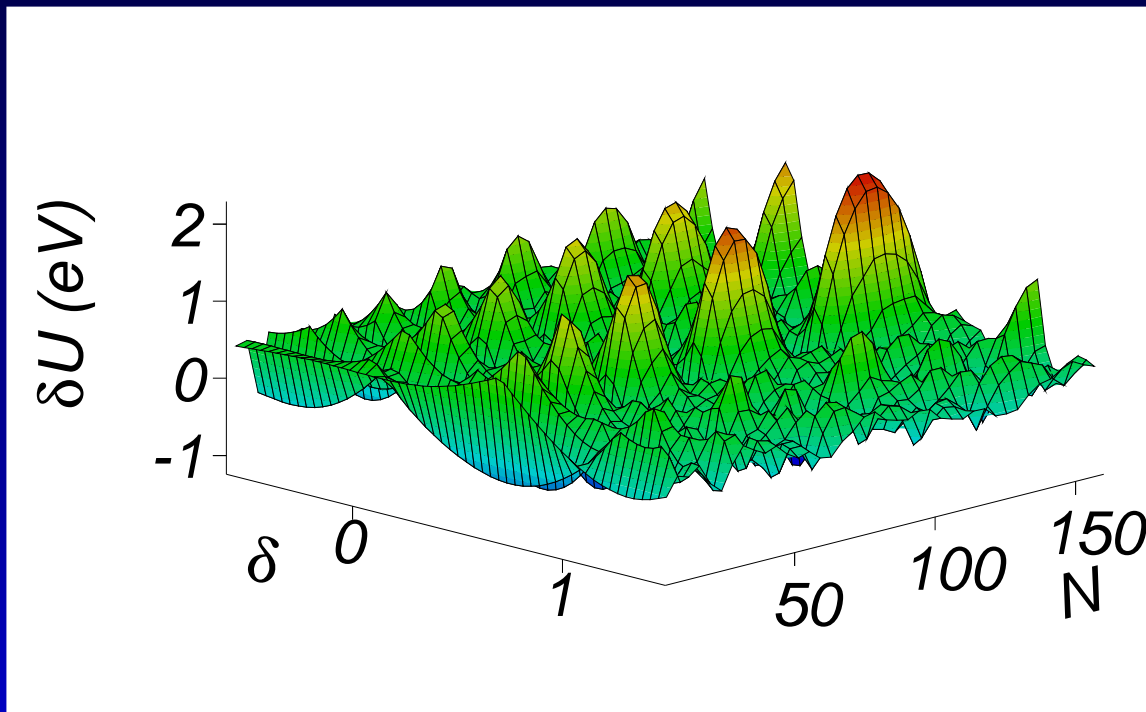
Pairing smoothing (right-hand side). 26 and 44 are hemispherical magic numbers; 56 is a mid-shell number.

M-MA hemisph. Na₁₄₈ cluster

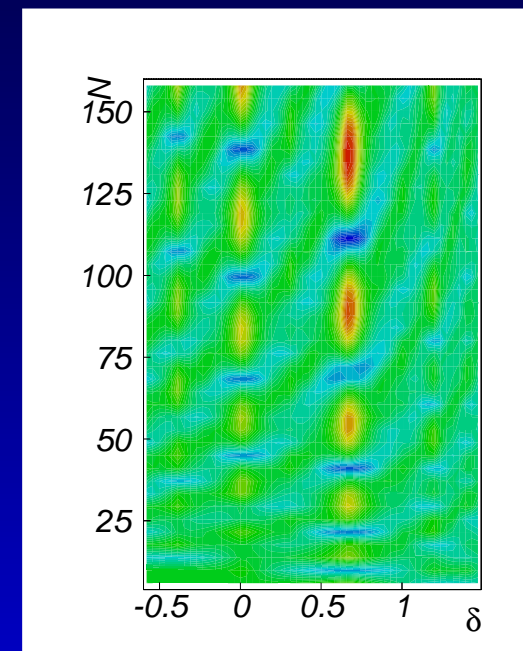


$E_v = -333$ eV was not included in E_{LD} and E . Liquid drop and total deformation energy (top), shell plus pairing corrections for hemispheroidal harmonic oscillator energy levels using the deformation parameter δ (bottom). Ground state shape prolate
 $\delta = 0.47$

Shell corrections hemispheroid



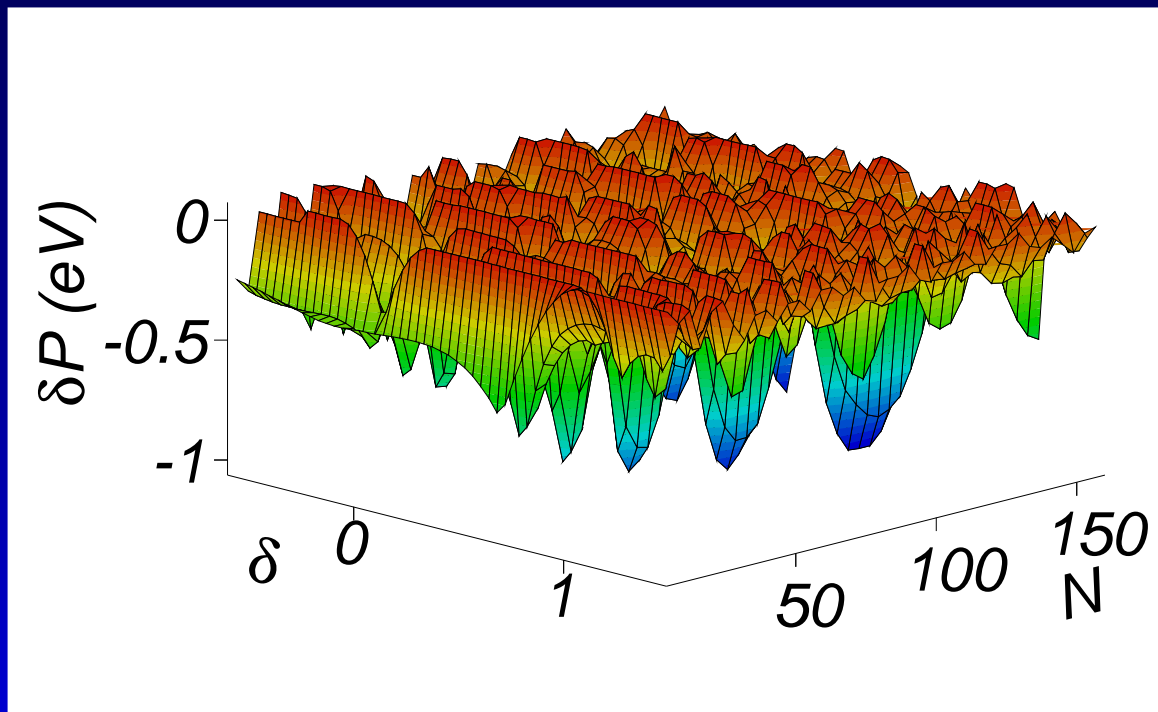
PES



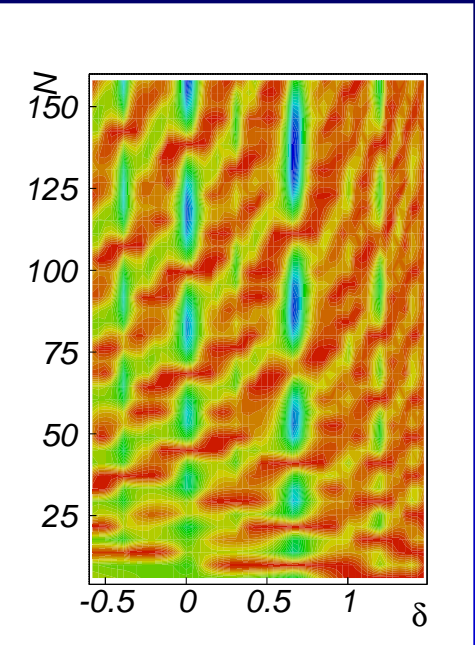
Contour plot

Pairing corr. hemispheroid

In a δ, N plane valleys and ridges are progressing parabolically

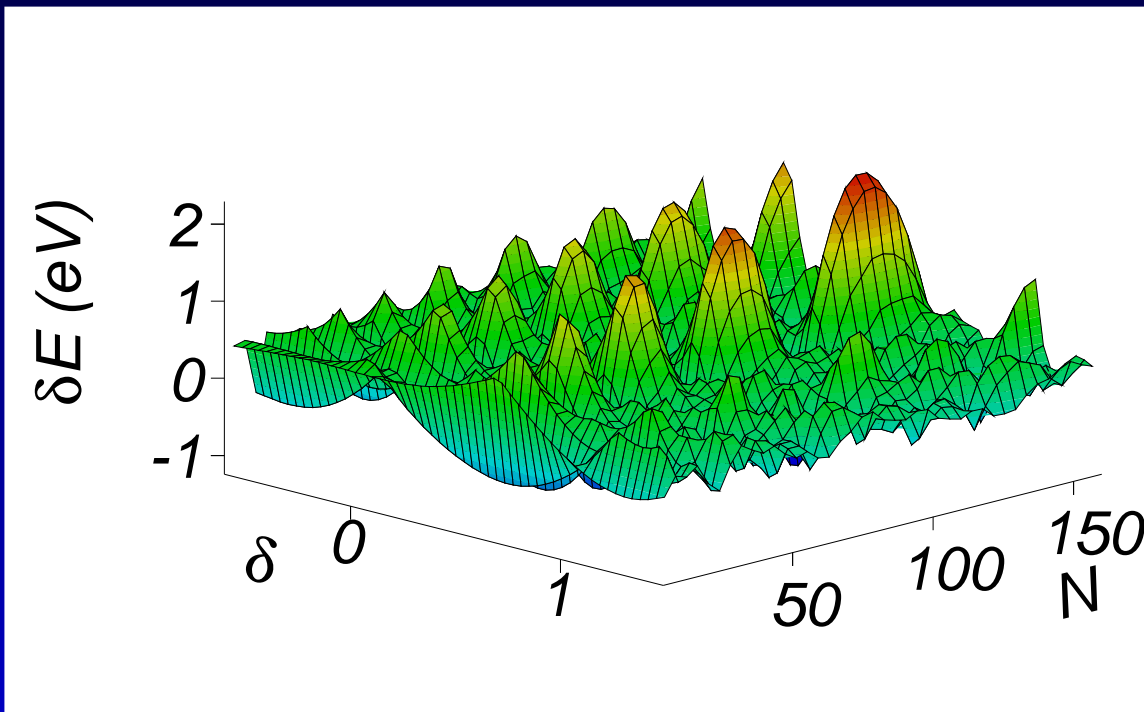


PES

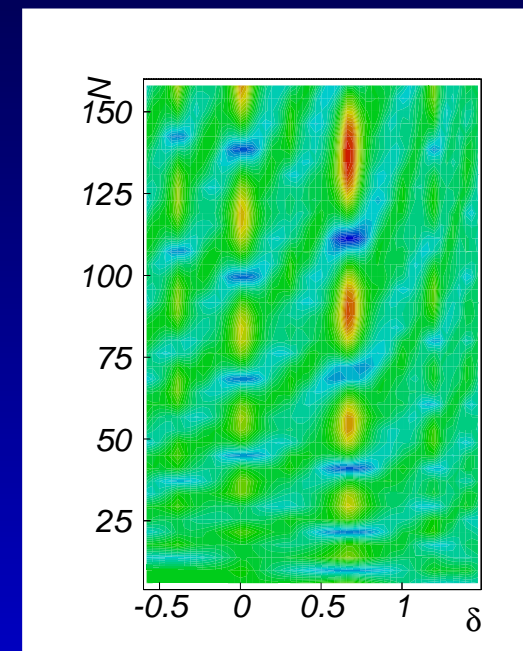


Contour plot

Shell+pairing corr. hemisph.



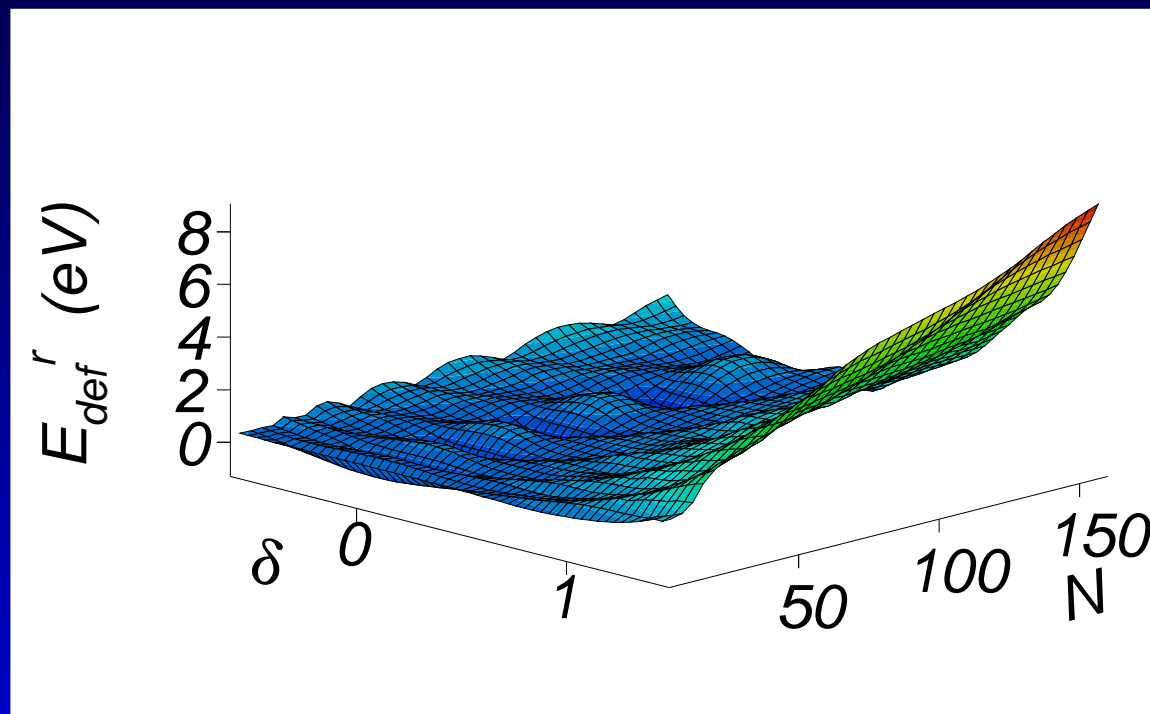
PES



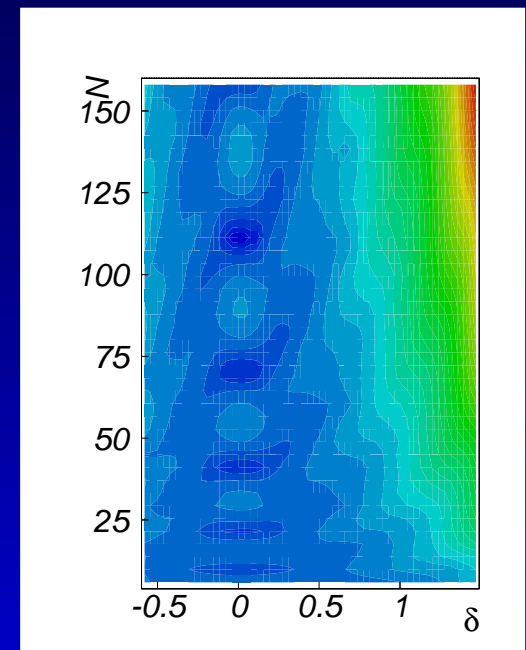
Contour plot

Total M-M rel. def. energy

$$E_{def}^r = E_{LD} - E_{LD}^0 + \delta E$$



PES



Contour plot

CONCLUSIONS I

- Neutral, free hemispheroidal clusters were investigated, as a 1st approx. to study cluster deposition on a surface
- They allow to obtain analytical results: surface, curvature deformation energy, shell model energies. Easy to interpret and short computer running time
- Within the LDM the most stable shape is a superdeformed prolate hemispheroid

CONCLUSIONS II

- A new hemispheroidal harmonic oscillator was derived.
 $Z(z)$ component of wave function has negative parity
- Its hemispherical ($\delta = 0$) magic numbers are identical with those obtained at the oblate spheroidal superdeformed shape: 2, 6, 14, 26, 44, 68, 100, 140, ...
- Maximum degeneracy at superdeformed ($\delta = 2/3$) prolate shape. Magic numbers identical with those of the spherical shape: 2, 8, 20, 40, 70, 112, 168 ...
- Pairing may be used to obtain smoother microscopic corrections
- In a δ, N plane shell corr., pairing corr. and total def. energy valleys and ridges are progressing parabolically

CONCLUSIONS III

- Interaction with the substrate was simulated by multiplying the surface tension of the base with a real number
 i = interaction factor
- Equilibrium shapes are
 - oblate hyperdeformed hemispheroids ($\delta = -1, a/c = 3$) when $i = -0.76$
 - superdeformed oblate semi-spheroid ($\delta = -0.68, a/c = 2$) when $i = -0.58$
 - hemisphere ($\delta = 0, c/a = 1$) when $i = 0$
 - superdeformed prolate semi-spheroid ($\delta = 0.63, c/a = 1.9$) when $i = 1$
 - prolate hyperdeformed hemispheroids ($\delta = 0.97, c/a = 2.9$) when $i = 2$
- The LDM was also applied to short and long spheroidal caps.

Published works

1. *D.N. Poenaru, R.A. Gherghescu, A.V. Solov'yov, W. Greiner*, Liquid drop stability of a superdeformed prolate semi-spheroidal atomic cluster, *EPL* **79** (2007) 63001.
2. *V.V. Semenikhina, A.G. Lyalin, A.V. Solov'yov, W. Greiner*, Droplet model of an atomic cluster at a solid surface, *J. Exp. Theor. Phys.* **106** (2008) 678-689.
3. *D.N. Poenaru, R.A. Gherghescu, I.H. Plonski, A.V. Solov'yov, W. Greiner*, Macroscopic-microscopic theory of semi-spheroidal atomic cluster, *Europ. Phys. J. D* **47** (2008) 379-393. HIGHLIGHT PAPER.
4. *D.N. Poenaru, R.A. Gherghescu, I.H. Plonski, A.V. Solov'yov, W. Greiner*, Potential energy surfaces of semi-spheroidal atomic clusters, *J. Phys.: Conf. Series* **111** (2008) 012047.
5. *D.N. Poenaru, R.A. Gherghescu, A.V. Solov'yov, W. Greiner*, Hemispheroidal quantum harmonic oscillator, *Physics Letters A* **372** (2008) 5448-5451.
6. *R.A. Gherghescu, D.N. Poenaru, A.V. Solov'yov, W. Greiner*, Deformed shell closures for light atomic clusters, *Internat. J. Mod. Phys. B* **22** (2008) 4917-4935.
7. *D.N. Poenaru, R.A. Gherghescu, A.V. Solov'yov, W. Greiner*, Oblate equilibrium shapes of hemispheroidal atomic clusters, *EPL* **88** (2009) 23002.
8. *D.N. Poenaru, R.A. Gherghescu, W. Greiner*, Special properties of ^{264}Fm and of atomic clusters emitting singly charged trimers, *J. Phys. G* **36** (2009) 125101.

Authors

D.N. Poenaru^{1,2}, R.A. Gherghescu^{1,2}, I.H. Plonski², A.V. Solov'yov¹, W. Greiner¹

¹*Frankfurt Institute for Advanced Studies (FIAS), J W Goethe University, Frankfurt am Main, Germany*
and

²*Horia Hulubei National Institute of Physics and Nuclear Engineering (IFIN-HH), Bucharest-Magurele, Romania*

